Supplementary Materials for

The Perfect Storm:

Gene Tree Estimation Error, Incomplete Lineage Sorting, and Ancient Gene

Flow Explain the Most Recalcitrant Ancient Angiosperm Clade, Malpighiales

Liming Cai*, Zhenxiang Xi, Emily Moriarty Lemmon, Alan R. Lemmon, Austin Mast,

Christopher E. Buddenhagen, Liang Liu, Charles C. Davis*

*Correspondence to: L.C. (lcai@g.harvard.edu) or C.C.D. (cdavis@oeb.harvard.edu)

This PDF file includes:

Supplementary Note 1

Inference of gene flow using phylogenetic invariant and

phylogenetic network methods

We applied three alternative introgression inference methods, including HyDe, quartetsampling, and PhyloNet_MPL, to our Malpighiales empirical data set and compared their performance to our method. HyDe is a phylogenetic invariant method that evaluates hypotheses of introgression based on site patterns in triplets. Quartetsampling tests introgression using quartet topology frequencies and uses Chi-square test to evaluate the statistical significance of deviation from the coalescent model. PhyloNet_MPL infers species networks using a maximum pseudolikelihood approach. We also applied a simulated data set to HyDe and quartetsampling to evaluate false positive rates (see also main text).

Methods

Application of empirical data

We applied our low-stringency data set to the three aforementioned methods. To run HyDe, we used the concatenated alignment of 423 loci in combination with the python command 'individual_hyde.py' to test all triplets. No additional parameter is required. To run quartetsampling, we used the concatenated alignment and the optimum MP-EST species tree inferred from the low-stringency data set (Fig. 3). The program was run with '--calc-qdstats --engine raxml --partitions' flags to use RAxML to infer the optimum topology for individual gene partitions and conduct Chi-square testing for quartet differential (QD) statistics. To run PhyloNet, we used the Bayesian gene trees inferred from the low-

stringency data set and reconstructed the network with one, two, and three reticulate

branches.

Application of simulated data

To evaluate the false positive rate of HyDe and quartetsampling, we applied the

simulated multi-locus alignments from the section *Simulation of gene alignments with*

realistic parameters of ILS and gene tree estimation error (see main text) to these two

methods. Briefly, gene trees were simulated based on the optimum MP-EST species tree

(Fig. 3) and then alignments were simulated for each gene tree. The coalescent and

mutational parameters used for simulation were inferred from the low-stringency data set,

reflecting high species divergence, low incomplete lineage sorting (theta = 0.01), and no

introgression. We sampled 423 alignments, each 400 bp in length to assemble a data set

that is similar in size. We then applied the concatenated alignment to HyDe and

quartetsampling following the methods described above.

Results

PhyloNet

PhyloNet_MPL generated inconsistent estimations among independent runs when

setting the number of reticulation events to be one, two, and three (Figs. S8-10). The log

probability for these inferences ranged from -1.0608e7 to -1.0598e7 and the network with

two reticulate branches received the highest log probability of -1.0598e7. Across these

three networks, the lineages involved in reticulate evolution and their phylogenetic

placements were highly variable (Figs. S8-10). These results highlight the challenges of network reconstruction when phylogenetic uncertainty is high.

HyDe

HyDe identified gene flow in 394 triplets (1.3%, Bonferroni corrected *p*-value 1.71×10^{-6}) in the empirical data set and only thirteen of them overlapped with the 553 triplets identified by our method. When mapping these 394 triplets back to the species tree, we found them to be randomly distributed across the phylogeny because the percentage of introgression triplets associated with most nodes is close to the global average of 1.3% except for few recently diverged clades including Pandaceae and Calophyllaceae (Fig. S11). Such random distribution is inconsistent with the pattern generated by gene flow in which the donor and recipient lineages are expected to be overrepresented in these triplets. In addition, in the simulated, gene-flow-free data set, HyDe reported gene flow in 2,417 triplets (Bonferroni corrected *p*-value 1.71×10^{-6}, Fig. 12), suggesting a false positive rate of 8.2%. The random distribution of introgression triplets from the empirical result and the high false positive rate of 8.2% from the simulation result indicate that the accuracy of HyDe is likely compromised by mutational noise and does not provide meaningful inference of gene flow for highly divergent species.

Quartetsampling

Quartetsampling yielded the most consistent estimations of gene flow compared to our result. In the empirical data set, significantly asymmetrical quartet frequency distributions were found in fifteen nodes (Chi-square test *p*-value <0.05). Eight of these

nodes are located within Clade 1 and Clade 2 (Fig. S13), which is consistent with our

findings using triplet distribution (Fig. 5c) and further supports our conclusion that these

two clades represent hotspots of reticulate evolution in Malpighiales. In addition,

quartetsampling also identified introgression along the backbone. We hypothesize that

these additionally identified nodes are more likely to represent false positives due to

phylogenetic uncertainty because four of the seven false positives from our simulation

reside in this area (Fig. S14). Several features of quartetsampling makes it potentially

sensitive to phylogenetic uncertainty: (1) It compares the frequency distribution of the two

discordant quartet topologies to evaluate the fitness of the coalescent model. When the

species tree is incorrectly reconstructed, one of the discordant quartets that reflect the true

species relationship will be dominant among gene trees. (2) The optimum quartet topology

is assessed based on sequences from four species rather than using the full taxon sampling,

which can be inaccurate due to limited taxon sampling. For example, when analyzing the

simulated data set, all quartets associated with the MRCA of Calophyllaceae and

Bonnetiaceae support only one of the two discordant topologies ($QC = -1$, $QD = 0$ in Fig.

S14), leading to a significantly skewed quartet frequency and rejection of the coalescent

model. But this is an artifact of an incorrectly inferred quartet topology due to limited

taxon sampling—when we inferred the species tree with full taxon sampling, the

concordant quartet topology is dominant and receives 100 bootstrap (BP) support (Fig.

S5a). Given that the majority of the false positives in Fig. S14 are distributed along the

backbone of the phylogeny, we conclude that quartetsamping is less robust to phylogenetic

uncertainty. In contrast, our triplet method compares the frequency difference between the

two less frequent triplets regardless of the topology of the species tree. Therefore, our

identification of gene flow in triplets is insensitive to phylogenetic uncertainty in the species tree.

Supplementary Note 2

Phylogenetic locus subsampling to assess nodal stability

Phylogenetic locus subsampling has become increasingly important as data sets scale to include entire genomes. The premise is that each gene carries unique properties of biological functions, evolutionary rate, and genealogical history that could complicate phylogenetic inference. Subsampling genes to more thoroughly investigate these properties can not only improve phylogenetic estimates by reducing noise (Salichos and Rokas 2013), but also allow for testing phylogenomic stability and potentially reveal insights into organismal biology (Edwards 2016).

Methods

We created subsampled data sets for assessing topological consistency between concatenation and coalescent methods. For each of our high/medium/low-stringency data sets, we ordered the loci separately by (i) alignment length, (ii) total number of parsimony informative (PI) sites, (iii) and gene tree robustness (measured by average ML BP). Each of these factors has been shown to influence the accuracy of phylogenetic reconstruction (Salichos and Rokas 2013). For (i), the subsampled data sets were created through the ordered addition of loci in the following bins: >600, 599–500, and 499–400 bp. This resulted in three subsampled alignments for each of our high/medium/low-stringency data sets. Similarly, for (ii) we ordered the loci based on number of PI sites (high to low) and for (iii) loci were ordered based on their inferred gene tree support (high to low). Upon

applying the latter two ordering strategies (ii and iii), we further down-sampled each of

these data sets to include 25%, 50%, and 75% of the ordered loci, respectively. This

resulted in twenty-seven subsampled data sets of varying sizes (Table S2). We then

conducted species tree inference based on each of the subsampled data sets using

concatenation and coalescent methods as described above (Table S2).

Results

We identified across all permutations of our three main data sets—whether

subsampling by locus length, number of PI sites, or average gene tree nodal support—that

the species trees estimated from the largest data set always produced a higher mean BP

support than subsampled data sets (Table S2). This applied for both our concatenation and

coalescent analyses. When filtering by locus length, the average species tree nodal support

inferred from each of the three largest data sets was significantly higher than nodal

support estimates for rival topologies derived from the subsampled data sets (p-value =

3.2e-3 in Student's t-test, Table S2). Similarly, subsampling by number of PI sites or gene

trees robustness also did not significantly improve the average species tree nodal support

(p-value = 3.9e-3 and 5.8e-4, respectively, Table S2).

References

Edwards, S.V., Xi, Z., Janke, A., Faircloth, B.C., McCormack, J.E., Glenn, T.C., Zhong, B., Wu, S.,
	Lemmon, E.M., Lemmon, A.R. 2016. Implementing and testing the multispecies
	coalescent model: a valuable paradigm for phylogenomics. Mol Phylogenet Evol,
	94:447-462.
Salichos, L., Rokas, A. 2013. Inferring ancient divergences requires genes with strong
	phylogenetic signals. Nature, 497:327-331.

Supplementary Note 3

Collapsing low support gene tree nodes for coalescent-based species tree estimation

Collapsing low support branches from gene trees has been demonstrated to be an effective method to mitigate gene tree estimation error and improve species tree estimation accuracy in coalescent methods (Zhang et al. 2017). We tested this approach by collapsing low support branches (< 10 BP support) and infering a species tree using ASTRAL-III (Zhang et al. 2017).

Methods

The input gene trees are estimated by RAxML using the low-stringency data set, which is the same as Analysis 16 in Table S2. We then applied newick utilities (Junier and Zdobnov 2010) to collapse all low supported nodes in the ML gene trees with BP support values lower than 10. This BP threshold is recommended in the ASTRAL-III manual (https://github.com/smirarab/ASTRAL/blob/master/astral-tutorial.md#running-with-unresolved-gene-trees) and was recently applied to a broad phylotranscriptomic analysis of green plants (One Thousand Plant Transcriptomes Initiative, 2019). We then inferred a species tree using ASTRAL-III v5.7.3 under the default setting using these collapsed ML gene trees. Finally, we quantified the overall gene tree–species tree discordance using the normalized quartet score inferred by ASTRAL. We also compared the average nodal posterior support between species trees estimated from collapsed gene trees and fully resolved gene trees.

Results

Collapsing gene tree nodes with less than 10 BP led to the removal of the majority of the nodes along the backbone. In this case, less than 19% of the genes are phylogenetically informative (BP >10) for these nodes. Collapsing low support nodes reduces gene tree–species tree discordance as expected, and the normalized quartet score increases from 0.508 to 0.797. However, we observed little improvement in species tree support and the average posterior support of the species tree increased only slightly from 0.945 to 0.946. Though topological conflicts are identified in 18 branches between the two species trees (Robinson-Foulds distance 0.14), none of these conflicts are well supported (posterior support <0.7). As a result, we conclude that collapsing low support branches in gene trees does not improve species tree support in our case.

References

Junier, T., Zdobnov, E.M. 2010. The Newick utilities: high-throughput phylogenetic tree processing in the UNIX shell. Bioinformatics, 26:1669-1670.

One Thousand Plant Transcriptomes Initiative. 2019. One thousand plant transcriptomes and the phylogenomics of green plants. Nature, 574:679.

Zhang, C., Sayyari, E., Mirarab, S. 2017. ASTRAL-III: increased scalability and impacts of contracting low support branches. RECOMB international workshop on comparative genomics, Springer, p. 53-75.

Supplementary Note 4

Inference of gene tree estimation error in the empirical data

We simulated DNA alignments to investigate the variation of gene tree estimation error in the empirical data sets. The simulation follows the same process described in the main manuscript except that we use the substitution model from each locus instead of the concatenated matrix. These results allow us to infer the natural range of gene tree estimation error in our empirical data, which we subsequently compared against our simulation analysis below to assess whether the later reflected a realistic scenario of gene tree estimation error in our empirical data.

Methods

Our simulation is based on gene trees inferred from the low-stringency data set since it represents our most data-rich matrix and also produced the most well supported species tree topology. We extracted the parameters of the GTR+Γ model from the RAxML log file for individual genes to simulate alignments of 300, 400, 500, 1000, and 1500 bp for all 423 loci using the program BppSeqGen in BppSuite v2.2.0 (Dutheil and Boussau 2008). We then applied RAxML to infer gene trees from the simulated data. Finally, the resulting gene trees from these simulated sequences were compared to the "true" gene trees (the trees initially inferred from the low-stringency data set) to quantify gene tree estimation error in our empirical data set. We measured gene tree estimation error using the RF distance (Robinson and Foulds 1981) by comparing the topological difference between estimated gene trees and the true gene trees.

Results

       Gene tree estimation error in empirical gene trees was inferred to be 0.313 for alignments of 300bp, 0.248 for 400bp, 0.204 for 500bp, 0.115 for 1000bp, and 0.083 for 1500bp (Fig. S4). Here, an RF distance of 0 signifies error-free reconstruction versus 1 indicating that none of the true nodes are recovered. When controlled for alignment length, the average gene tree estimation error in all of our simulation was significantly higher than that estimated from the empirical data (p-value= 4.24e-65 in Student's t-test, Fig. S4).
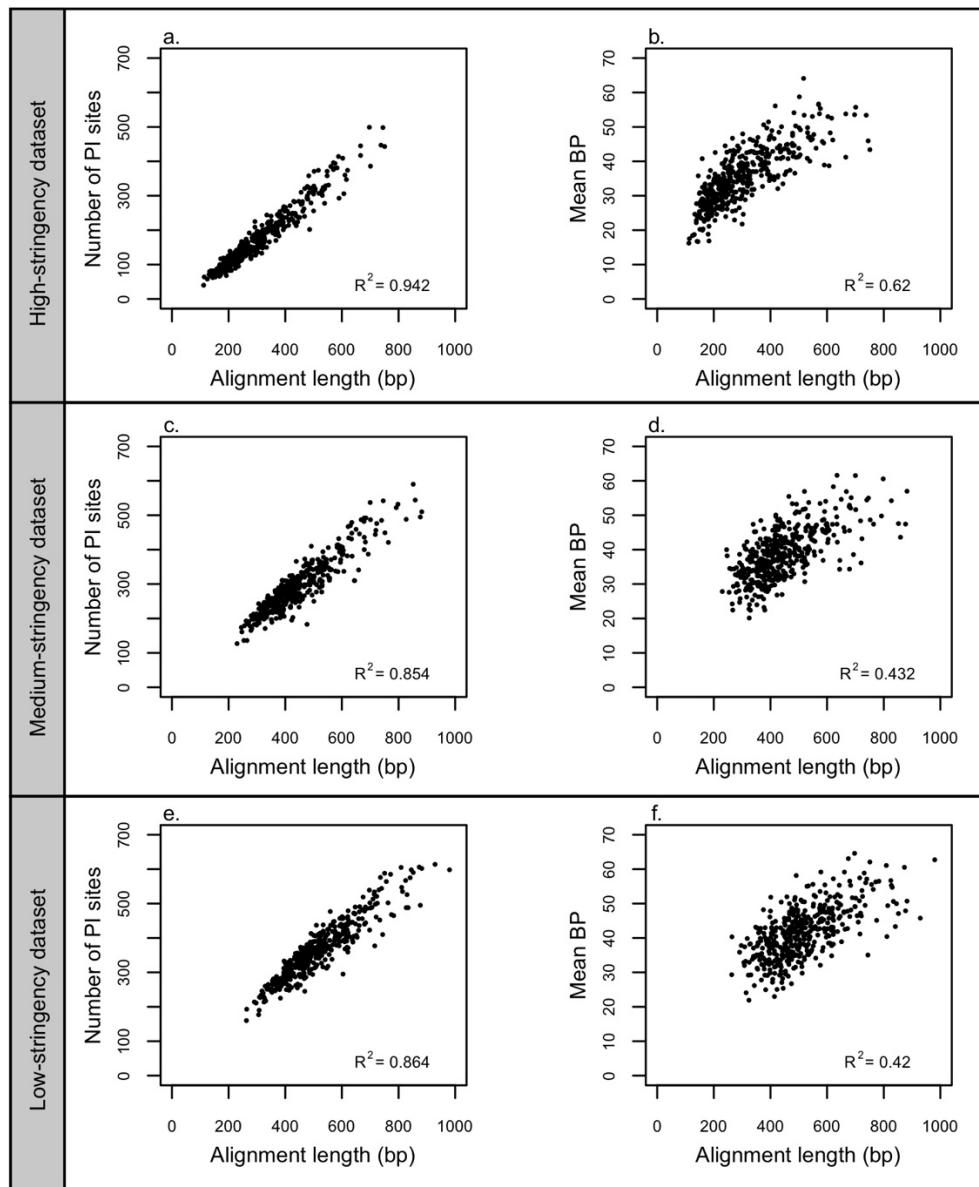
Figure S1 Number of parsimony informative (PI) sites and mean gene tree bootstrap support (BP) is positively correlated with alignment length in high/medium/low-stringency data sets. (a,b) Correlation between number of PI sites (a) or mean gene tree BP (b) with alignment lengths inferred from the high-stringency data set. (c,d) Correlation between number of PI sites (c) or mean gene tree BP (d) with alignment lengths inferred from the medium-stringency data set. (e,f) Correlation between number of PI sites (e) or mean gene tree BP (f) with alignment lengths inferred from low-stringency data set. Pearson's R^2 is presented at lower right corner of each plot.
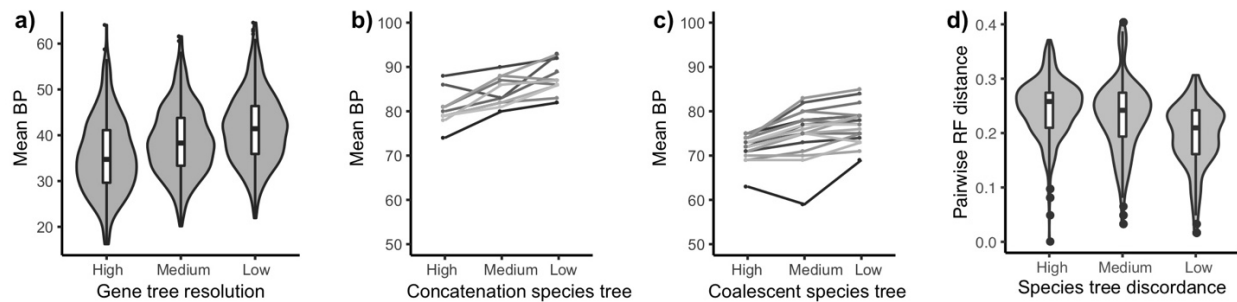
Figure S2 Increased gene tree and species tree support as more flanking sites are included in the analysis. The low-stringency data set contains the highest proportion of flanking regions and also has the highest gene tree and species tree bootstrap support (BP). (a) Distribution of mean gene tree support in high/medium/low-stringency data sets. (b,c) Increased species tree support in concatenation (b) and coalescent analyses (c). Analyses with same locus subsampling are connected by lines (see Supplementary Note 2 and Table S2 for details). (d) Increased species tree inference consistency reflected by pairwise Robinson-Foulds (RF) distance. High = High-stringency data; Medium = Medium-stringency data; Low = Low-stringency data.
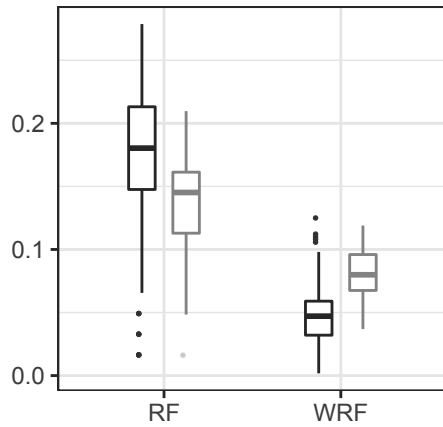
Figure S3 Species tree estimation discordance is higher in concatenation analyses (grey) than coalescent (black) when using various site and locus subsampling strategies. Y-axis is the pairwise species tree distance measured by Robinson-Foulds (RF) distance or weighted RF distance (WRF, weighted by nodal support). Left, distribution of pairwise RF distances among species trees estimated from 62 coalescent analyses (black) and 36 concatenation analyses (grey). Right, distribution of pairwise WRF distances distances among species trees estimated from 62 coalescent analyses (black) and 36 concatenation analyses (grey). See Table S2 for detailed methods description for the 98 analyses.
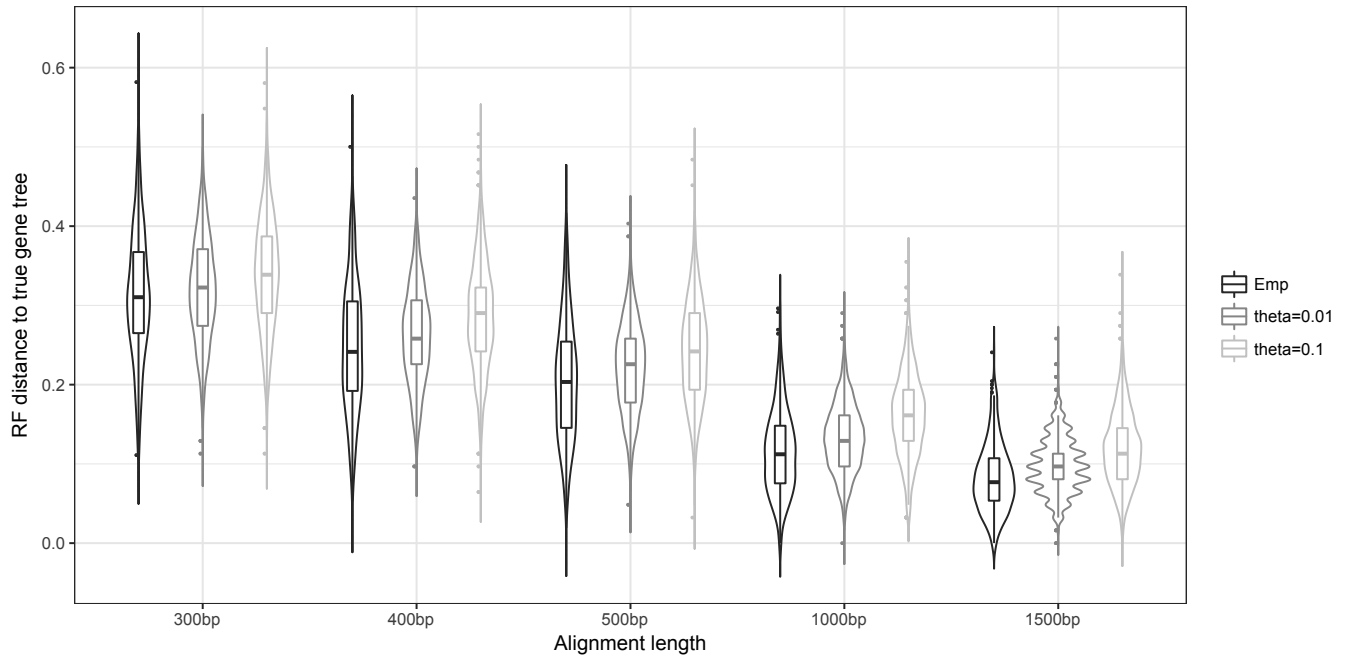
Figure S4 Gene tree estimation errors in empirical and simulated data are negatively correlated with alignment length. For both empirical and simulated data sets, gene tree estimation error is measured by Robinson-Foulds (RF) distance between the estimated gene trees to the 'true gene trees'. For the empirical (emp) data, alignments were first simulated based on the *empirical* gene trees. For the simulated data, alignments were simulated based on the *simulated* gene trees under low (theta=0.01) and high (theta=0.1) levels of incomplete lineage sorting. Then RAxML gene trees are inferred based on these simulated alignments and compared to the true gene trees. See Supplementary Note 4 for detailed method description.
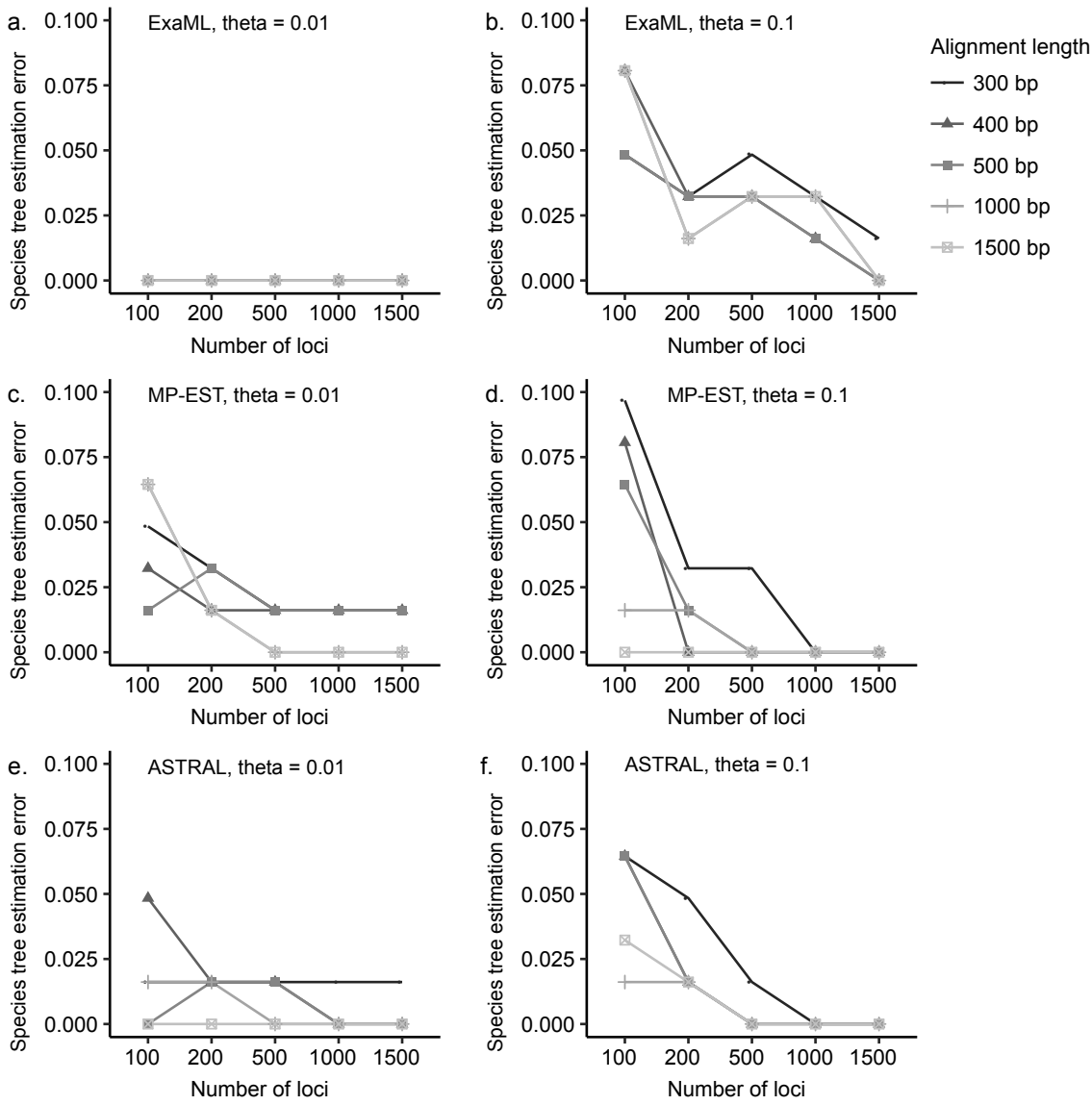
Figure S5 Species tree estimation error in simulated data sets under low (theta = 0.01) and high (theta=0.1) levels of incomplete lineage sorting using concatenation and coalescent methods. Species tree estimation error is measured by Robinson-Foulds (RF) distance from inferred species tree in each analysis to the known species tree. Results derived from alignments of varying lengths (300, 400, 500, 1000, 1500 bp) are marked by different shape and different shades of grey. (a,b) Species tree estimation error using concatenation method (ExaML) under low (a) and high (b) ILS. (c,d) Species tree estimation error using coalescent method (MP-EST) under low (c) and high (d) ILS. (e,f) Species tree estimation error using coalescent method (ASTRAL-II) under low (e) and high (f) ILS.
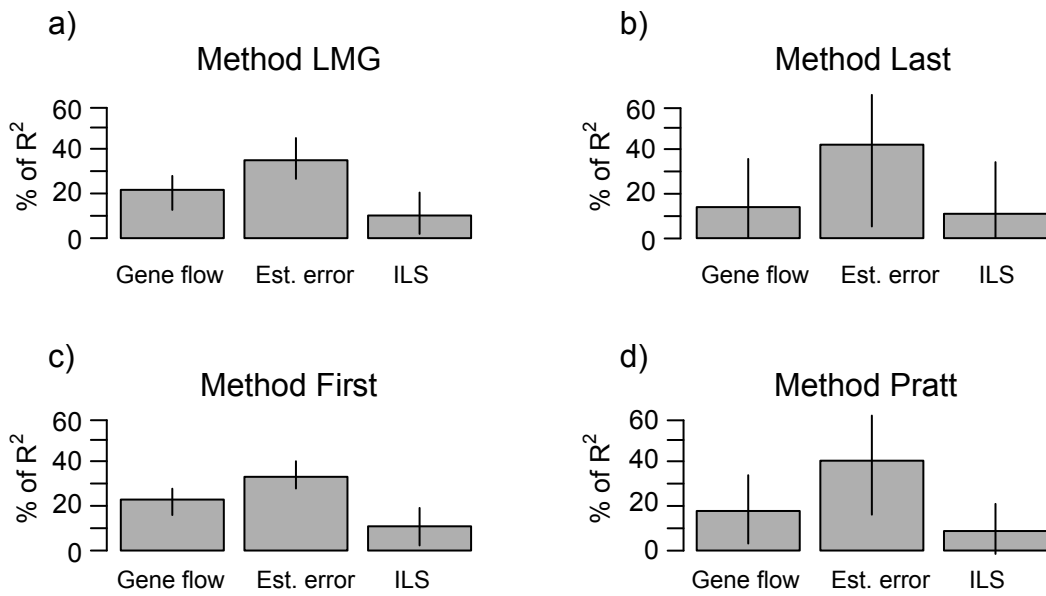
Figure S6 Relative importance of incomplete lineage sorting (ILS), gene tree estimation error (Est. error), and gene flow in generating gene tree variation. The percentages are estimated based on four regression methods (LMG, Last, First, and Pratt) implemented in the R package *relaimpo*. 95% confidence intervals are represented by bars. All four methods support gene tree estimation error as the major factor leading to gene tree variation in Malpighiales.
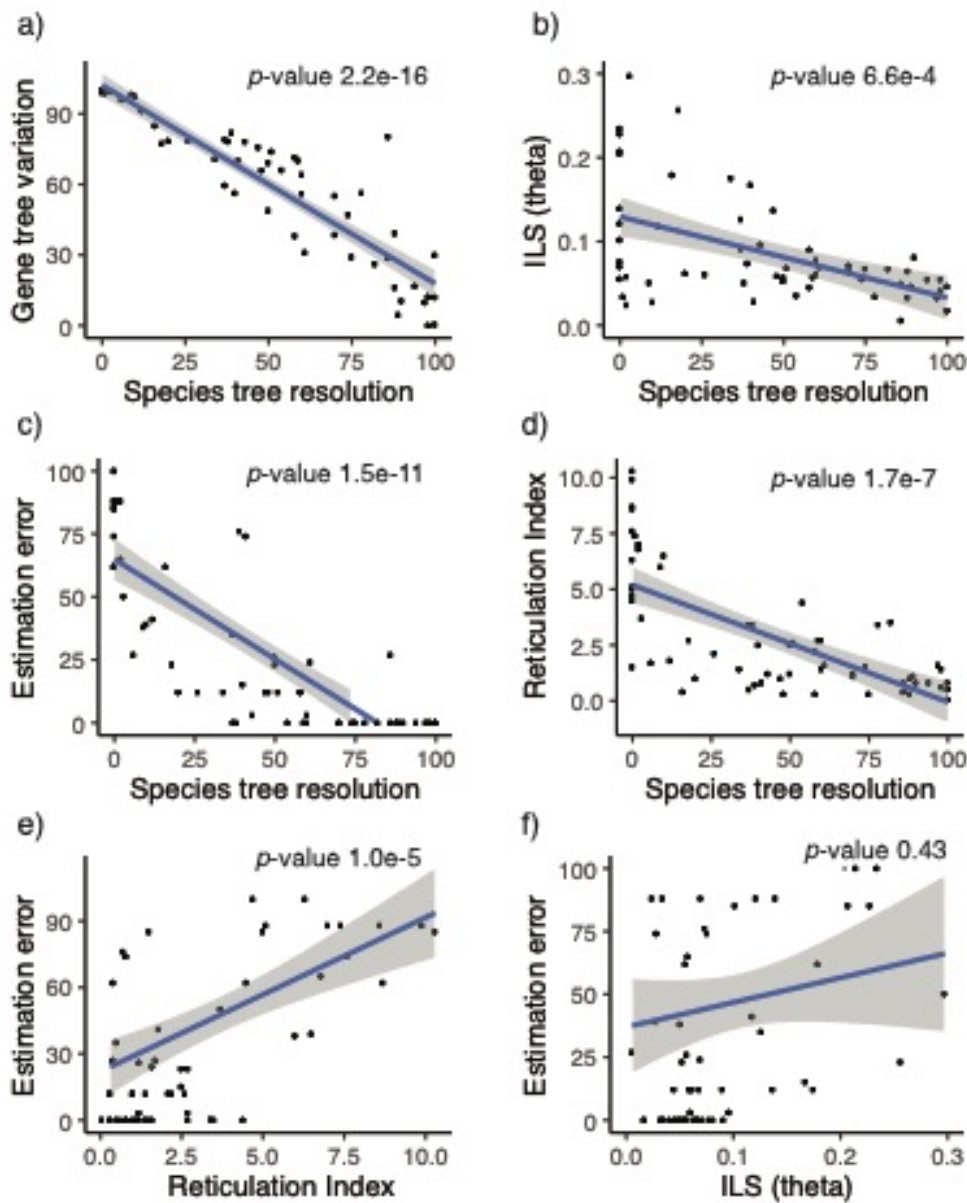
Figure S7 ILS, gene tree estimation error, and introgression contribute to low species tree support in Malpighiales. Species tree support is represented by nodal support from the MP-EST phylogeny in Fig. 3 from the main text. The other statistics reflect the variables presented in Figure 5, including incomplete lineage sorting (ILS), gene tree estimation error, and introgression. The *p*-value of the Pearson's correlation test is indicated in the upper right corner in each panel. (a) Significant negative correlation between gene tree variation and species tree support. (b) Significant negative correlation between ILS (measured by population polymorphism parameter theta) and species tree support. (c)

(Figure S7 continued) Significant negative correlation between gene tree estimation error and species tree support. (d) Significant negative correlation between introgression (measured by Reticulation Index) and species tree support. (e) Significant positive correlation between gene tree estimation error and introgression. (f) No significant correlation between gene tree estimation error and ILS.
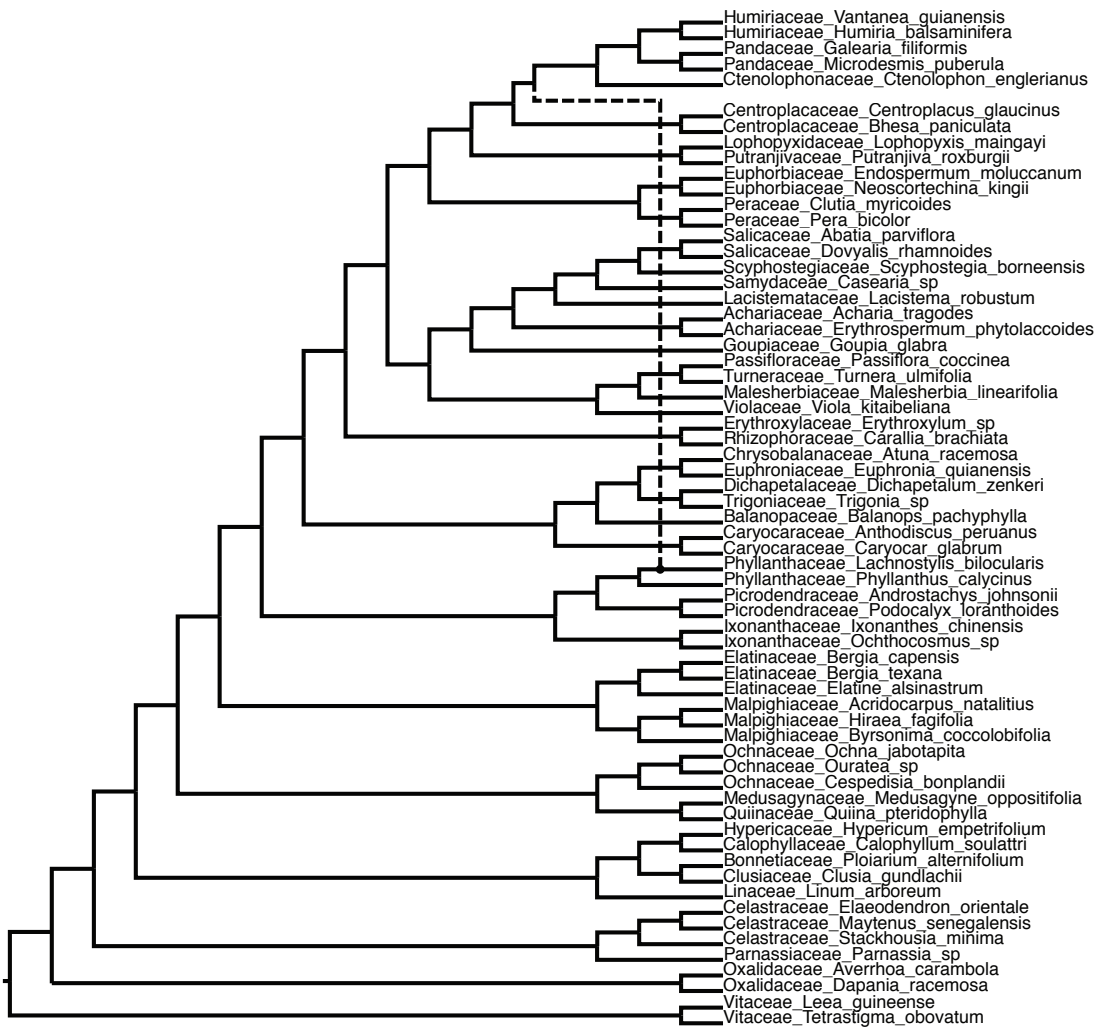
Figure S8 Species network reconstruction of Malpighiales allowing for one reticulation. The dotted line indicates the two lineages involved in reticulation evolution. The network is inferred using the maximum pseudo-likelihood method implemented in PhyloNet based on 423 RAxML gene trees from the low-stringency data set. A starting species tree topology estimated by MP-EST in Fig. 3 is used. Total log probability is -1.0608e7.
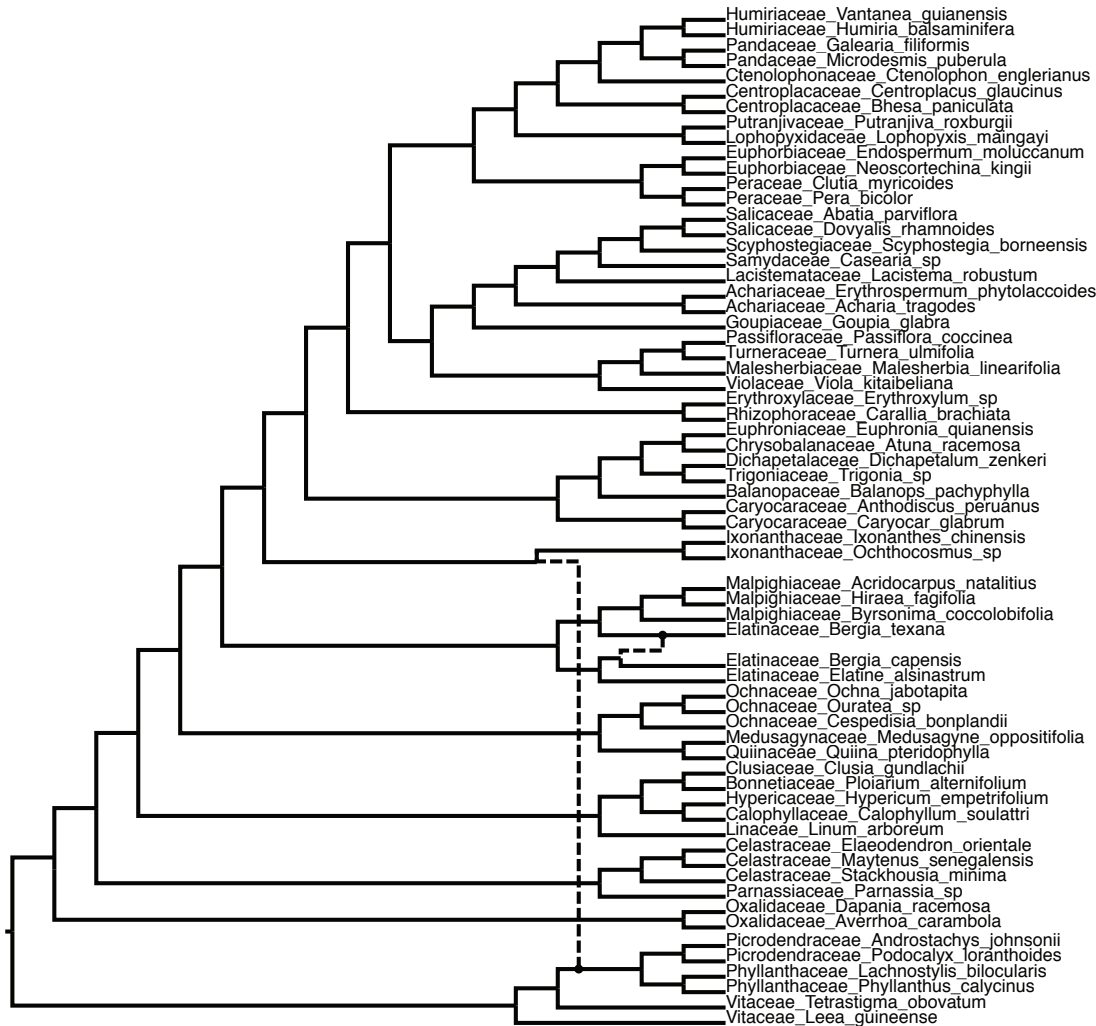
Figure S9 Species network reconstruction of Malpighiales allowing for two reticulations. Each dotted line indicates the two lineages involved in reticulation evolution. The network is inferred using the maximum pseudo-likelihood method implemented in PhyloNet based on 423 RAxML gene trees from the low-stringency data set. A starting species tree topology estimated by MP-EST in Fig. 3 is used. Total log probability is -1.0598e7.
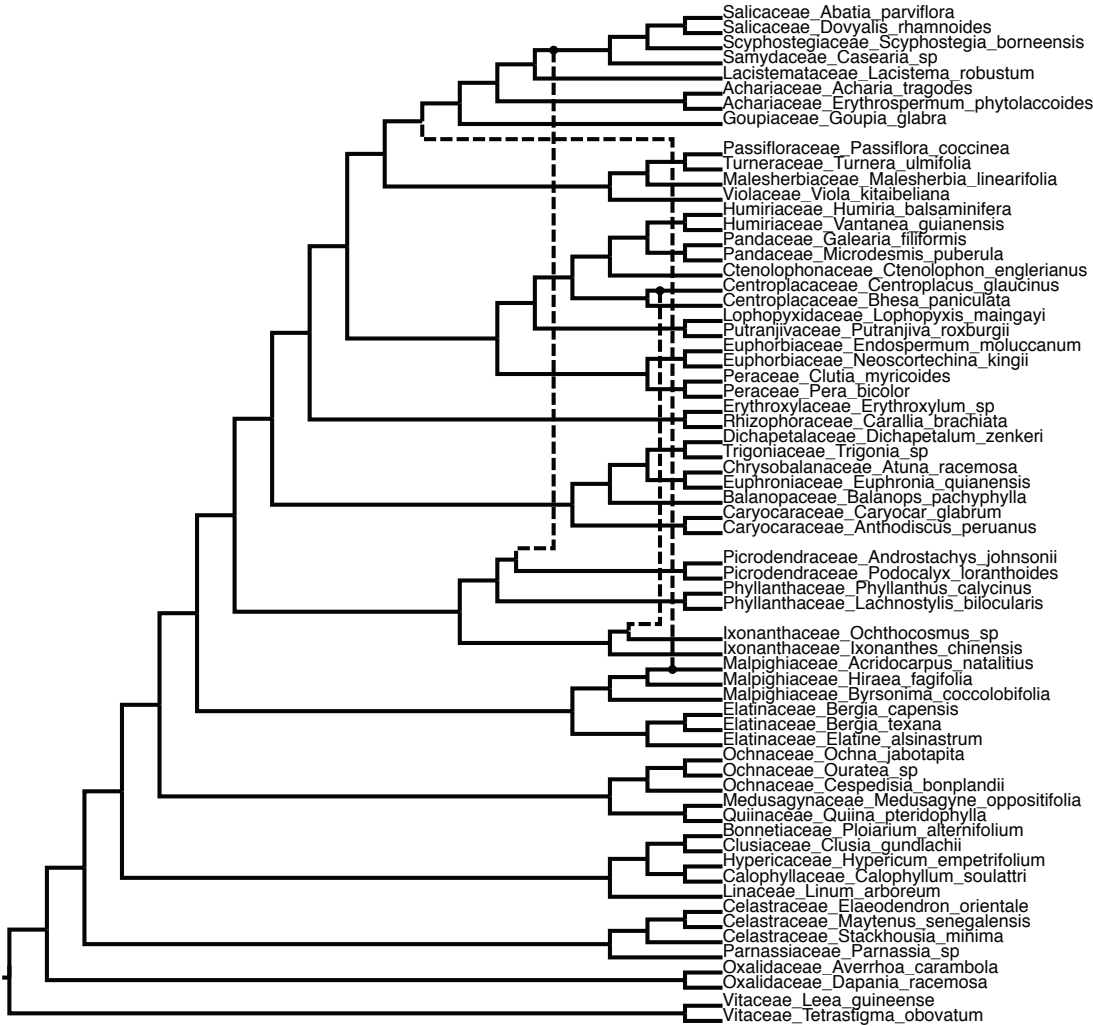
Figure S10 Species network reconstruction of Malpighiales allowing for three reticulations. Each dotted line indicates the two lineages involved in reticulation evolution. The network is inferred based on 423 RAxML gene trees from the low-stringency data set using the maximum pseudo-likelihood method implemented in PhyloNet. A starting species tree topology estimated by MP-EST in Fig. 3 is used. Total log probability is -1.0604e7.
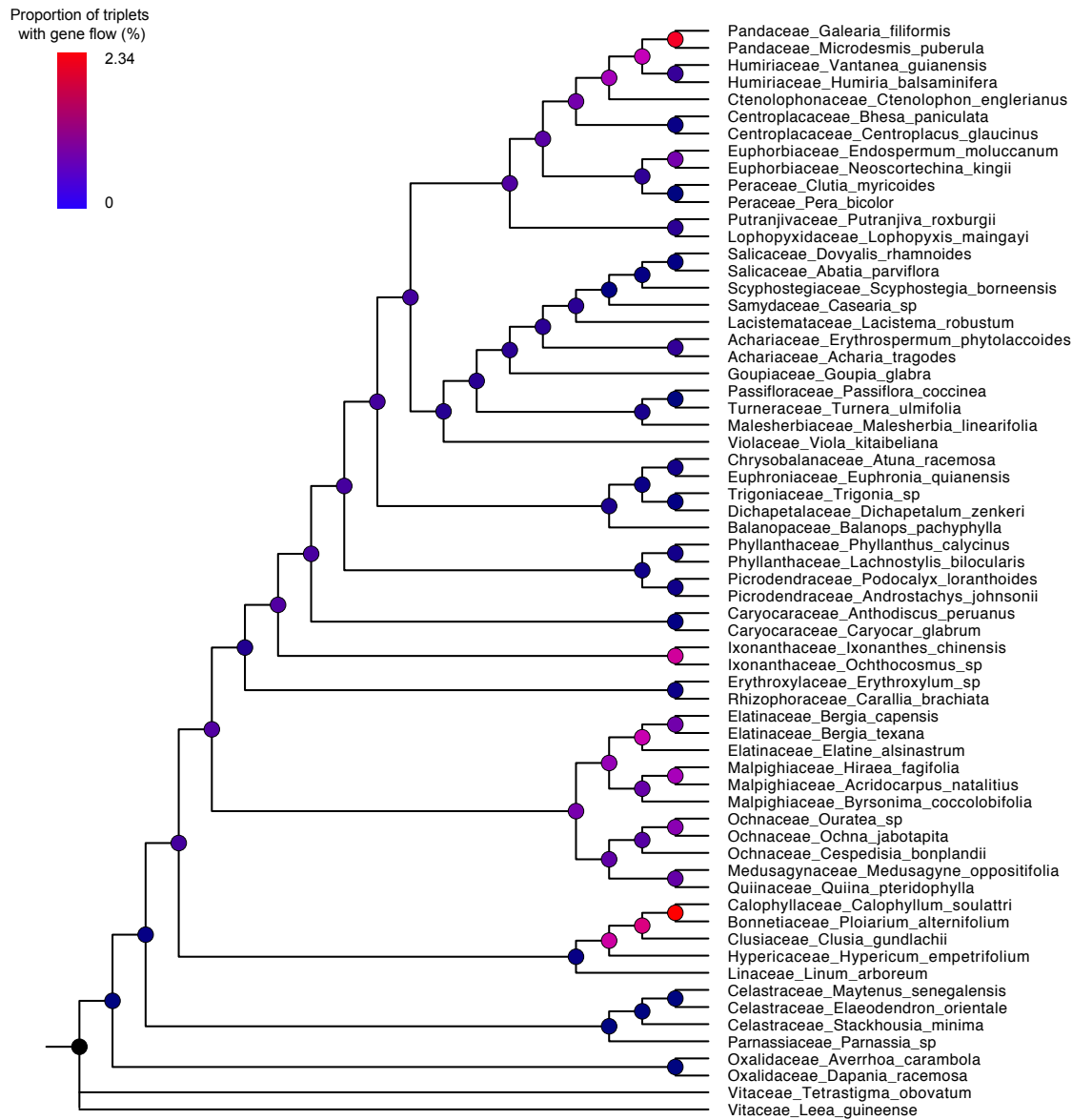
Figure S11 Identification of gene flow in the empirical data set of Malpighiales using HyDe. HyDe identified significant (Bonferroni corrected *p*-value 1.71×10^{-6}, Chi-square test) gene flow in 394 triplets (1.3%) based on the low-stringency data set, which were mapped to the optimum MP-EST species tree from Fig. 3 to visualize their phylogenetic distribution. Internal nodes are colored based on the proportion of triplets with significant gene flow identified by HyDe, which is similar to the calculation of Reticulation Index of our method in Fig. 5c.
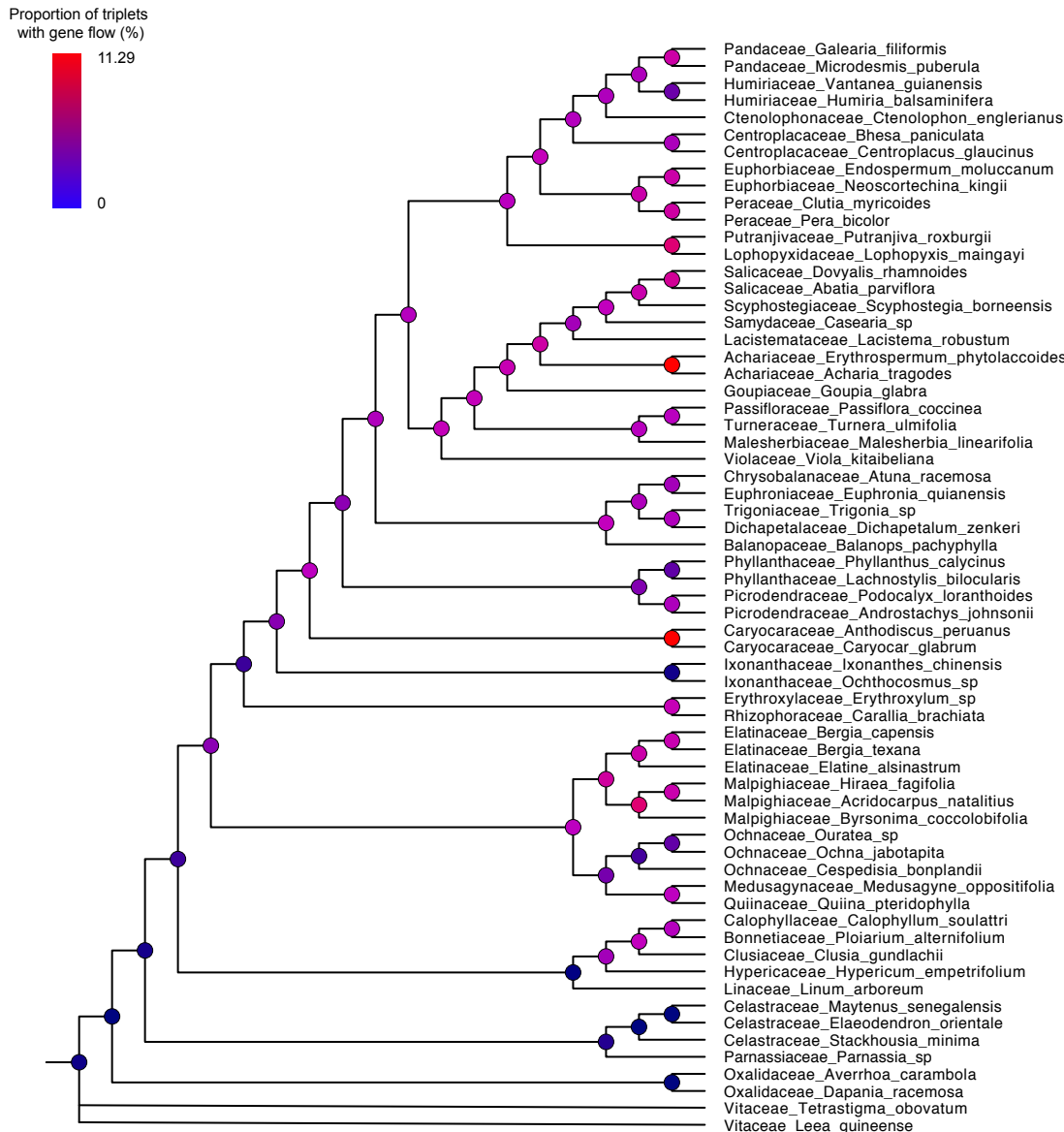
Figure S12 Evaluating false positive rate of HyDe using simulated data set. HyDe identified significant gene flow (Bonferroni corrected *p*-value 1.71×10⁻⁶, Chi-square test) in 2,417 triplets in a simulated, gene-flow-free alignment, suggesting a false positive rate of 8.2%. This simulated data set is generated based on the mutational and coalescent parameters estimated from the low-stringency data set of Malpighiales. See Supplementary Note 1 for detailed method description. These 2,417 triplets were mapped to the optimum MP-EST species tree from Fig. 3 to visualize their phylogenetic distribution. Internal nodes are colored based on the proportion of triplets with significant gene flow identified by HyDe, which is similar to the calculation of Reticulation Index of our method in Fig. 5c.
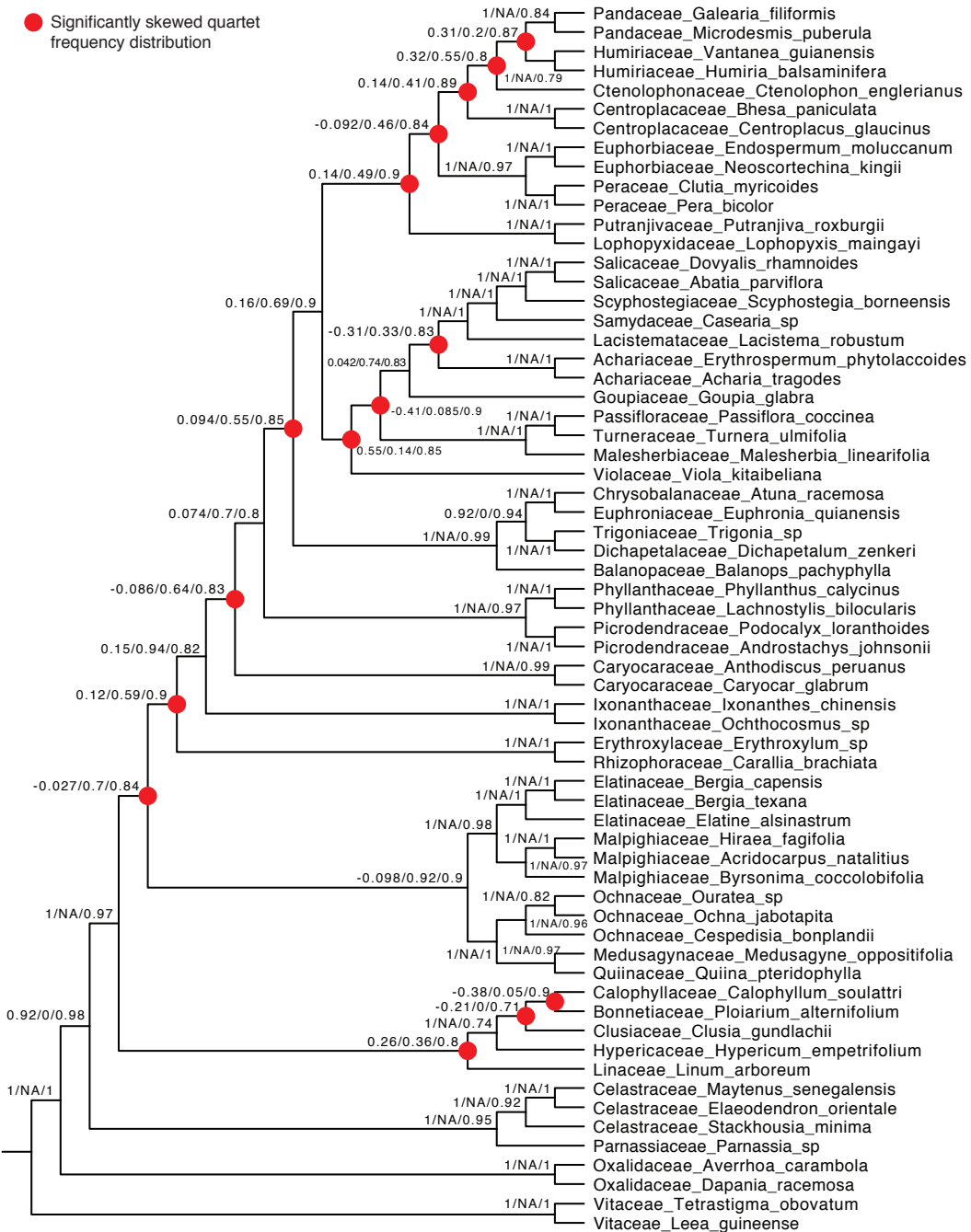
Figure S13 Identification of gene flow in the empirical data set of Malpighiales using quartetsampling. Nodes with significantly skewed Quartet Differential score (QD, *p*-value <0.05, Chi-square test) are associated with gene flow and highlighted in red. The quartetsampling analysis is conducted based on the concatenated alignment of the low-stringency data set using 100 replicates. Quartet Concordance (QC)/QD/Quartet Informativeness (QI) scores are shown on the branch for each node. Here, QC quantifies the

(Figure S13 continued) frequency of the concordant topology among replicates, QD measures the disparity between the two discordant topologies, and QI quantifies the proportion of well-supported quartet tree.
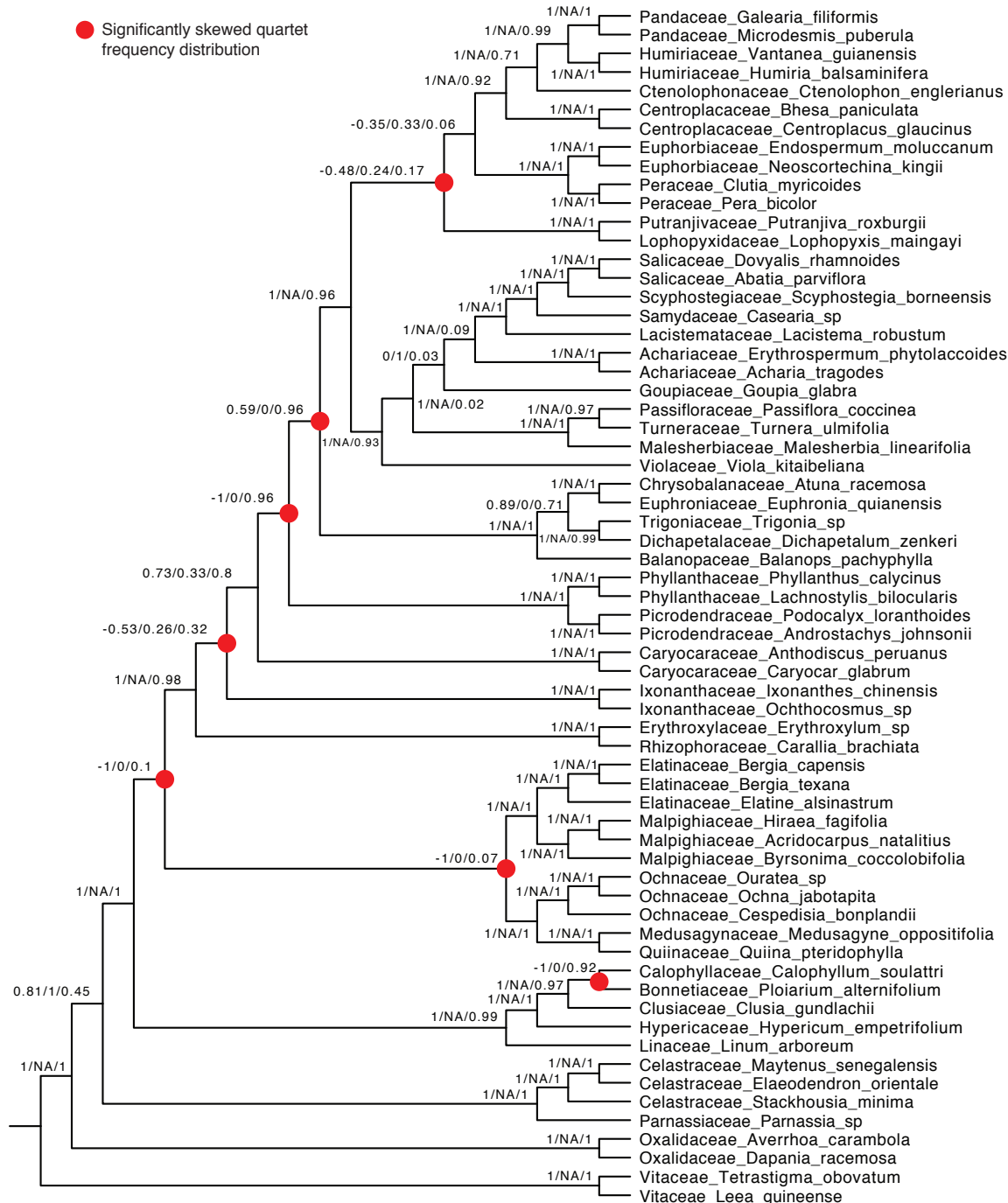
Figure S14 Evaluating the false positive rate of quartetsampling in gene flow identification. We applied quartetsampling to a simulated, gene-flow-free data set. This simulated data set is generated based on the mutational and coalescent parameters estimated from the low-stringency data set of Malpighiales. Eight nodes with significantly skewed Quartet Differential scored (QD, *p*-value <0.05, Chi-square test) are falsely identified with

(Figure S14 continued) introgression and highlighted in red. Quartet Concordance (QC)/ Quartet Differential (QD)/Quartet Informativeness (QI) scores estimated by quartetsampling are shown on the branch. See Supplementary Note 1 for detailed method description. Here, QC quantifies the frequency of the concordant topology among replicates, QD measures the disparity between the two discordant topologies, and QI quantifies the proportion of well-supported quartet tree.

Table S1 Voucher and GenBank information for 64 species in Malpighiales, Celastrales, Oxalidales, and Vitales used for anchored hybrid enrichment. Vouchers indicated as 'Xi et al. 2012' are plant materials used in Xi et al. (2012).

Library ID	Order	Family	Species	Voucher
I10347_CP89	Vitales	Vitaceae	*Leea guineense*	Xi et al. 2012
I10351_CP95	Vitales	Vitaceae	*Tetrastigma obovatum*	Xi et al. 2012
I8629_573	Oxalidales	Oxalidaceae	*Dapania racemosa*	Ambri & Arifin 1014 (K; 2/1992)
I8628_572	Oxalidales	Oxalidaceae	*Averrhoa carambola*	Chase 214 (NCU)
I8653_KW795	Celastrales	Parnassiaceae	*Parnassia sp*	Wurdack D795 (US)
I8612_254	Celastrales	Celastraceae	*Stackhousia minima*	B. P. J. Molloy s.n. (CHR)
I8607_242	Celastrales	Celastraceae	*Maytenus senegalensis*	Collenette 4/93 (K)
I8604_226	Celastrales	Celastraceae	*Elaeodendron orientale*	M. W. Chase 1213 (K)
I8623_350	Malpighiales	Caryocaraceae	*Caryocar glabrum*	Mori 22997 (NY)
I8645_CP61	Malpighiales	Caryocaraceae	*Anthodiscus peruanus*	Xi et al. 2012
I8602_221	Malpighiales	Linaceae	*Linum arboreum*	M. W. Chase 478 (K)
I8598_217	Malpighiales	Clusiaceae	*Clusia gundlachii*	M. W. Chase 341 (NCU)
I8656_SM324	Malpighiales	Bonnetiaceae	*Ploiarium alternifolium*	S. M. 324
I8613_257	Malpighiales	Calophyllaceae	*Calophyllum soulattri*	M. W. Chase 1217 (K)
I8597_216	Malpighiales	Hypericaceae	*Hypericum empetrifolium*	M. W. Chase 837 (K)
I8649_CP70	Malpighiales	Medusagynaceae	*Medusagyne oppositifolia*	Xi et al. 2012
I8608_245	Malpighiales	Quiinaceae	*Quiina pteridophylla*	J. Murça Pires (CPATU)
I8610_248	Malpighiales	Ochnaceae	*Cespedisia bonplandii*	M. W. Chase 1325 (K)
I10338_CP78	Malpighiales	Ochnaceae	*Ochna jabotapita*	Xi et al. 2012
I10330_CP26	Malpighiales	Ochnaceae	*Ouratea sp*	Xi et al. 2012
I8626_570	Malpighiales	Ixonanthaceae	*Ixonanthes chinensis*	Zhiduan Chen 9812087
I8652_KW534	Malpighiales	Ixonanthaceae	*Ochthocosmus sp*	Berry 6561 (MO)
I13012_633	Malpighiales	Malpighiaceae	*Byrsonima coccolobifolia*	WRA 13661
I8668_690	Malpighiales	Malpighiaceae	*Hiraea fagifolia*	WRA 13593
I10364_2649	Malpighiales	Malpighiaceae	*Acridocarpus natalitius*	K. Peterson UConn 199500164

I13020_2310	Malpighiales	Elatinaceae	*Elatine alsinastrum*	Unto Laine, Tapio Lammes, Jaakko Nurmi (NY)
I10383_2253	Malpighiales	Elatinaceae	*Bergia capensis*	G.E. Crow 6068a (MO)
I8638_2169	Malpighiales	Elatinaceae	*Bergia texana*	Zhang, Ahart, and Bartholomew 84 (A)
I8646_CP63	Malpighiales	Ctenolophonaceae	*Ctenolophon englerianus*	Xi et al. 2012
I8631_576	Malpighiales	Rhizophoraceae	*Carallia brachiata*	Chase 2151 (K)
I8634_928	Malpighiales	Erythroxylaceae	*Erythroxylum sp*	Andre Amorim 3964
I8644_CP60	Malpighiales	Balanopaceae	*Balanops pachyphylla*	Xi et al. 2012
I8603_222	Malpighiales	Euphroniaceae	*Euphronia quianensis*	Mori 23699 (NY)
I8616_261	Malpighiales	Chrysobalanaceae	*Atuna racemosa*	M. W. Chase 2118 (K)
I8647_CP64	Malpighiales	Trigoniaceae	*Trigonia sp*	Xi et al. 2012
I8643_CP59	Malpighiales	Dichapetalaceae	*Dichapetalum zenkeri*	Xi et al. 2012
I8615_260	Malpighiales	Phyllanthaceae	*Phyllanthus calycinus*	M. W. Chase 2163 (K)
I8614_259	Malpighiales	Phyllanthaceae	*Lachnostylis bilocularis*	M. W. Chase 1960 (K)
I8606_241	Malpighiales	Picrodendraceae	*Androstachys johnsonii*	M. W. Chase 1904 (K)
I8648_CP66	Malpighiales	Picrodendraceae	*Podocalyx loranthoides*	Xi et al. 2012
I8651_KW143	Malpighiales	Lophopyxidaceae	*Lophopyxis maingayi*	Adelbai P-10203 (US)
I8611_251	Malpighiales	Putranjivaceae	*Putranjiva roxburgii*	FTG 83463A (K)
I10353_WHZ5	Malpighiales	Centroplacaceae	*Bhesa paniculata*	Zhang and Boufford 160 (A)
I8654_KW1098	Malpighiales	Centroplacaceae	*Centroplacus glaucinus*	White 128, ser. 1 (MO)
I8599_218	Malpighiales	Violaceae	*Viola kitaibeliana*	M. W. Chase 6173 (K)
I8622_346	Malpighiales	Achariaceae	*Erythrospermum phytolaccoides*	M. W. Chase 1277 (K)
I8593_212	Malpighiales	Achariaceae	*Acharia tragodes*	Chase 812 (NCU)
I8617_262	Malpighiales	Goupiaceae	*Goupia glabra*	Prevost 3031 (CAY)
I8624_354	Malpighiales	Malesherbiaceae	*Malesherbia linearifolia*	M. W. Chase 609 (K)
I8600_219	Malpighiales	Passifloraceae	*Passiflora_coccinea*	M. W. Chase 2475 (K)
I8601_220	Malpighiales	Turneraceae	*Turnera_ulmifolia*	M. W. Chase 220 (NCU)
I10329_CP24	Malpighiales	Lacistemataceae	*Lacistema_robustum*	Xi et al. 2012
I8655_MA26	Malpighiales	Samydaceae	*Casearia_sp*	Xi et al. 2012

I8620_342	Malpighiales	Scyphostegiaceae	*Scyphostegia_borneensis*	J. Davis (BH)
I8619_341	Malpighiales	Salicaceae	*Dovyalis_rhamnoides*	M. W. Chase 271 (NCU)
I8618_340	Malpighiales	Salicaceae	*Abatia_parviflora*	R. T. Pennington 676
I8595_214	Malpighiales	Humiriaceae	*Humiria_balsaminifera*	W. R. Anderson 13654 (MICH)
I8594_213	Malpighiales	Humiriaceae	*Vantanea_guianensis*	Pennington 13855 (K)
I8621_344	Malpighiales	Pandaceae	*Microdesmis_puberula*	M. Cheek 5986 (K)
I8633_734	Malpighiales	Pandaceae	*Galearia_filiformis*	Chase 1334 (K)
I8637_1347	Malpighiales	Peraceae	*Clutia_myricoides*	Taku Miyazaki 991013R2 (A)
I8650_KW041	Malpighiales	Peraceae	*Pera_bicolor*	Gillespie 4300 (US)
I8632_733	Malpighiales	Euphorbiaceae	*Neoscortechina_kingii*	Chase 1265 (K)
I8605_237	Malpighiales	Euphorbiaceae	*Endospermum_moluccanum*	M. W. Chase 1258 (K)

Table S2 Species tree estimation strategies using various phylogenetic estimation methods and phylogenetic subsampling methods (see Supplementary Note 2) with high-, medium-, and low-stringency data sets.

Analysis ID	Site subsampling details	Locus subsampling details	Species tree estimation method	Software for (gene tree) species tree estimation	Number of loci	Average nodal support	Marginal likelihood
1	High stringency dataset	complete dataset	Concatenation	RAxML	423	88	-2597883.4
2	High stringency dataset	complete dataset	Concatenation	EXaML	423	86	-2451009.2
3	High stringency dataset	complete dataset	Concatenation	PhyloBayes	423	0.82	NA
4	High stringency dataset	complete dataset	Coalescent	(RAxML) + MP-EST	423	75	NA
5	High stringency dataset	complete dataset	Coalescent	(RAxML) + ASTRAL	423	74	NA
6	Medium stringency dataset	complete dataset	Concatenation	RAxML	423	90	-4549339.8
7	Medium stringency dataset	complete dataset	Concatenation	EXaML	423	83	-4299274.2
8	Medium stringency dataset	complete dataset	Concatenation	PhyloBayes	423	0.82	NA
9	Medium stringency dataset	complete dataset	Coalescent	(RAxML) + MP-EST	423	78	NA
10	Medium stringency dataset	complete dataset	Coalescent	(RAxML) + ASTRAL	423	83	NA
11	Low stringency dataset	complete dataset	Concatenation	RAxML	423	92	-6046462.1
12	Low stringency dataset	complete dataset	Concatenation	EXaML	423	93	-5805350.2
13	Low stringency dataset	complete dataset	Concatenation	PhyloBayes	423	0.85	NA
14	Low stringency dataset	complete dataset	Coalescent	(RAxML) + MP-EST	423	79	NA
15	Low stringency dataset	complete dataset	Coalescent	(MrBayes) + MP-EST	423	87	NA
16	Low stringency dataset	complete dataset	Coalescent	(RAxML) + ASTRAL	423	85	NA
17	Low stringency dataset	complete dataset	Coalescent	(MrBayes) + ASTRAL	423	91	NA
Additional phylogenetic subsampling analyses (see Supplementary Note 1)							
18	High stringency dataset	alignment longer than 500bp	Concatenation	EXaML	38	74	-454160.66
19	High stringency dataset	alignment longer than 400bp	Concatenation	EXaML	82	80	-856659.66
20	High stringency dataset	alignment longer than 300bp	Concatenation	EXaML	180	81	-1534860.3
21	High stringency dataset	25% loci with most PI sites	Concatenation	EXaML	106	79	-1052819.1
22	High stringency dataset	50% loci with most PI sites	Concatenation	EXaML	212	81	-1735141
23	High stringency dataset	75% loci with most PI sites	Concatenation	EXaML	317	81	-2166192.4

24	High stringency dataset	25% loci with highest mean BP support	Concatenation	EXaML	106	79	-982245.41
25	High stringency dataset	50% loci with highest mean BP support	Concatenation	EXaML	212	78	-1646733.2
26	High stringency dataset	75% loci with highest mean BP support	Concatenation	EXaML	317	79	-2133478.1
27	High stringency dataset	alignment longer than 600bp	Coalescent	(RAxML) + MP-EST	38	63	NA
28	High stringency dataset	alignment longer than 500bp	Coalescent	(RAxML) + MP-EST	82	69	NA
29	High stringency dataset	alignment longer than 400bp	Coalescent	(RAxML) + MP-EST	180	71	NA
30	High stringency dataset	25% loci with most PI sites	Coalescent	(RAxML) + MP-EST	106	70	NA
31	High stringency dataset	50% loci with most PI sites	Coalescent	(RAxML) + MP-EST	212	72	NA
32	High stringency dataset	75% loci with most PI sites	Coalescent	(RAxML) + MP-EST	317	73	NA
33	High stringency dataset	25% loci with highest mean BP support	Coalescent	(RAxML) + MP-EST	106	69	NA
34	High stringency dataset	50% loci with highest mean BP support	Coalescent	(RAxML) + MP-EST	212	72	NA
35	High stringency dataset	75% loci with highest mean BP support	Coalescent	(RAxML) + MP-EST	317	73	NA
36	High stringency dataset	alignment longer than 600bp	Coalescent	(RAxML) + ASTRAL	38	71	NA
37	High stringency dataset	alignment longer than 500bp	Coalescent	(RAxML) + ASTRAL	82	72	NA
38	High stringency dataset	alignment longer than 400bp	Coalescent	(RAxML) + ASTRAL	180	74	NA
39	High stringency dataset	25% loci with most PI sites	Coalescent	(RAxML) + ASTRAL	106	73	NA
40	High stringency dataset	50% loci with most PI sites	Coalescent	(RAxML) + ASTRAL	212	74	NA
41	High stringency dataset	75% loci with most PI sites	Coalescent	(RAxML) + ASTRAL	317	75	NA
42	High stringency dataset	25% loci with highest mean BP support	Coalescent	(RAxML) + ASTRAL	106	72	NA
43	High stringency dataset	50% loci with highest mean BP support	Coalescent	(RAxML) + ASTRAL	212	74	NA
44	High stringency dataset	75% loci with highest mean BP support	Coalescent	(RAxML) + ASTRAL	317	75	NA
45	Medium stringency dataset	alignment longer than 600bp	Concatenation	EXaML	43	80	-616647.82
46	Medium stringency dataset	alignment longer than 500bp	Concatenation	EXaML	109	83	-1393081.9
47	Medium stringency dataset	alignment longer than 400bp	Concatenation	EXaML	256	87	-2914565
48	Medium stringency dataset	25% loci with most PI sites	Concatenation	EXaML	106	82	-1397259.3

49	Medium stringency dataset	50% loci with most PI sites	Concatenation	EXaML	212	88	-2545584.5
50	Medium stringency dataset	75% loci with most PI sites	Concatenation	EXaML	317	88	-3494618.8
51	Medium stringency dataset	25% loci with highest mean BP support	Concatenation	EXaML	106	82	-1308456.1
52	Medium stringency dataset	50% loci with highest mean BP support	Concatenation	EXaML	212	86	-2405398
53	Medium stringency dataset	75% loci with highest mean BP support	Concatenation	EXaML	317	81	-3386839.6
54	Medium stringency dataset	alignment longer than 600bp	Coalescent	(RAxML) + MP-EST	43	59	NA
55	Medium stringency dataset	alignment longer than 500bp	Coalescent	(RAxML) + MP-EST	109	71	NA
56	Medium stringency dataset	alignment longer than 400bp	Coalescent	(RAxML) + MP-EST	256	75	NA
57	Medium stringency dataset	25% loci with most PI sites	Coalescent	(RAxML) + MP-EST	106	70	NA
58	Medium stringency dataset	50% loci with most PI sites	Coalescent	(RAxML) + MP-EST	212	75	NA
59	Medium stringency dataset	75% loci with most PI sites	Coalescent	(RAxML) + MP-EST	317	76	NA
60	Medium stringency dataset	25% loci with highest mean BP support	Coalescent	(RAxML) + MP-EST	106	69	NA
61	Medium stringency dataset	50% loci with highest mean BP support	Coalescent	(RAxML) + MP-EST	212	75	NA
62	Medium stringency dataset	75% loci with highest mean BP support	Coalescent	(RAxML) + MP-EST	317	77	NA
63	Medium stringency dataset	alignment longer than 600bp	Coalescent	(RAxML) + ASTRAL	43	73	NA
64	Medium stringency dataset	alignment longer than 500bp	Coalescent	(RAxML) + ASTRAL	109	77	NA
65	Medium stringency dataset	alignment longer than 400bp	Coalescent	(RAxML) + ASTRAL	256	82	NA
66	Medium stringency dataset	25% loci with most PI sites	Coalescent	(RAxML) + ASTRAL	106	75	NA
67	Medium stringency dataset	50% loci with most PI sites	Coalescent	(RAxML) + ASTRAL	212	78	NA
68	Medium stringency dataset	75% loci with most PI sites	Coalescent	(RAxML) + ASTRAL	317	80	NA
69	Medium stringency dataset	25% loci with highest mean BP support	Coalescent	(RAxML) + ASTRAL	106	75	NA
70	Medium stringency dataset	50% loci with highest mean BP support	Coalescent	(RAxML) + ASTRAL	212	78	NA
71	Medium stringency dataset	75% loci with highest mean BP support	Coalescent	(RAxML) + ASTRAL	317	80	NA
72	Low stringency dataset	alignment longer than 600bp	Concatenation	EXaML	95	82	-1586587.8
73	Low stringency dataset	alignment longer than 500bp	Concatenation	EXaML	199	89	-3101987.3

74	Low stringency dataset	alignment longer than 400bp	Concatenation	EXaML	354	86	-5108938.3
75	Low stringency dataset	25% loci with most PI sites	Concatenation	EXaML	106	83	-1808049
76	Low stringency dataset	50% loci with most PI sites	Concatenation	EXaML	212	87	-3354963.3
77	Low stringency dataset	75% loci with most PI sites	Concatenation	EXaML	317	93	-4694879.8
78	Low stringency dataset	25% loci with highest mean BP support	Concatenation	EXaML	106	86	-1657659.5
79	Low stringency dataset	50% loci with highest mean BP support	Concatenation	EXaML	212	87	-3216469.8
80	Low stringency dataset	75% loci with highest mean BP support	Concatenation	EXaML	317	86	-4506786.8
81	Low stringency dataset	alignment longer than 600bp	Coalescent	(RAxML) + MP-EST	95	69	NA
82	Low stringency dataset	alignment longer than 500bp	Coalescent	(RAxML) + MP-EST	199	75	NA
83	Low stringency dataset	alignment longer than 400bp	Coalescent	(RAxML) + MP-EST	354	79	NA
84	Low stringency dataset	25% loci with most PI sites	Coalescent	(RAxML) + MP-EST	106	71	NA
85	Low stringency dataset	50% loci with most PI sites	Coalescent	(RAxML) + MP-EST	212	76	NA
86	Low stringency dataset	75% loci with most PI sites	Coalescent	(RAxML) + MP-EST	317	79	NA
87	Low stringency dataset	25% loci with highest mean BP support	Coalescent	(RAxML) + MP-EST	106	73	NA
88	Low stringency dataset	50% loci with highest mean BP support	Coalescent	(RAxML) + MP-EST	212	73	NA
89	Low stringency dataset	75% loci with highest mean BP support	Coalescent	(RAxML) + MP-EST	317	77	NA
90	Low stringency dataset	alignment longer than 600bp	Coalescent	(RAxML) + ASTRAL	95	74	NA
91	Low stringency dataset	alignment longer than 500bp	Coalescent	(RAxML) + ASTRAL	199	78	NA
92	Low stringency dataset	alignment longer than 400bp	Coalescent	(RAxML) + ASTRAL	354	84	NA
93	Low stringency dataset	25% loci with most PI sites	Coalescent	(RAxML) + ASTRAL	106	75	NA
94	Low stringency dataset	50% loci with most PI sites	Coalescent	(RAxML) + ASTRAL	212	79	NA
95	Low stringency dataset	75% loci with most PI sites	Coalescent	(RAxML) + ASTRAL	317	82	NA
96	Low stringency dataset	25% loci with highest mean BP support	Coalescent	(RAxML) + ASTRAL	106	75	NA
97	Low stringency dataset	50% loci with highest mean BP support	Coalescent	(RAxML) + ASTRAL	212	77	NA
98	Low stringency dataset	75% loci with highest mean BP support	Coalescent	(RAxML) + ASTRAL	317	79	NA

Table S3 Coalescent and mutational parameters of simulated data sets.

Data set ID	Level of ILS (theta)	Alignment length (bp)	Number of loci
1	0.01	300	100
2	0.01	300	200
3	0.01	300	500
4	0.01	300	1000
5	0.01	300	1500
6	0.01	400	100
7	0.01	400	200
8	0.01	400	500
9	0.01	400	1000
10	0.01	500	1500
11	0.01	500	100
12	0.01	500	200
13	0.01	500	500
14	0.01	500	1000
15	0.01	500	1500
16	0.01	1000	100
17	0.01	1000	200
18	0.01	1000	500
19	0.01	1000	1000
20	0.01	1000	1500
21	0.01	1500	100
22	0.01	1500	200
23	0.01	1500	500
24	0.01	1500	1000
25	0.01	1500	1500
26	0.1	300	100
27	0.1	300	200
28	0.1	300	500
29	0.1	300	1000
30	0.1	300	1500
31	0.1	400	100
32	0.1	400	200
33	0.1	400	500
34	0.1	400	1000
35	0.1	500	1500
36	0.1	500	100
37	0.1	500	200

38	0.1	500	500
39	0.1	500	1000
40	0.1	500	1500
41	0.1	1000	100
42	0.1	1000	200
43	0.1	1000	500
44	0.1	1000	1000
45	0.1	1000	1500
46	0.1	1500	100
47	0.1	1500	200
48	0.1	1500	500
49	0.1	1500	1000
50	0.1	1500	1500

Table S4 Summary statistics of 423 loci in high/medium/low-stringency data sets, including number of captured taxa, alignment length, number of PI sites, and mean gene tree BP.

Locus ID	Number of taxa	High-stringency data set			Medium-stringency data set			Low-stringency data set		
		Alignment length (bp)	Number of PI sites	Mean BP	Alignment length (bp)	Number of PI sites	Mean BP	Alignment length (bp)	Number of PI sites	Mean BP
T78_L1	59	466	262	42.5178571	604	387	43.01786	706	489	46.46429
T78_L100	62	291	187	38.440678	424	318	41.61017	494	388	43.27119
T78_L101	61	152	79	28.1724138	256	179	34.55172	291	214	35.86207
T78_L102	60	436	245	40.8070175	533	341	39.59649	615	423	42.21053
T78_L103	57	166	76	22.5740741	352	259	23.98148	445	352	25.38889
T78_L104	60	224	111	30.3157895	392	226	38.29825	453	287	38.01754
T78_L105	57	326	165	37.1111111	406	250	39.94444	463	307	42.35185
T78_L106	52	166	79	30.9795918	366	240	29.12245	459	325	33.30612
T78_L108	59	302	193	34.2321429	429	284	39.21429	490	345	39.51786
T78_L109	56	433	282	44.5849057	624	434	44.20755	672	482	47.77358
T78_L11	56	222	136	32.1320755	314	223	31.90566	355	264	34.98113
T78_L110	56	268	163	37.0188679	448	322	46.64151	522	396	47.9434
T78_L111	58	158	76	27.6909091	269	184	29.34545	312	227	33.21818
T78_L112	51	292	150	41.25	449	273	39	519	342	45.22917
T78_L113	61	382	241	38.3103448	400	266	42.7069	454	320	45.60345
T78_L114	58	337	220	39.6909091	426	285	39.56364	469	328	40.74545
T78_L115	58	183	81	21.1272727	307	191	31.69091	384	268	32.8
T78_L116	52	246	167	42.6530612	416	304	46.83673	476	364	48.42857
T78_L117	61	332	203	42.8965517	424	287	46.5	467	330	47.56897
T78_L118	59	247	155	27.4464286	314	208	28.53571	355	249	30.91071
T78_L119	64	531	313	49.7868853	563	342	47.13115	610	389	52
T78_L121	62	400	210	34.7627119	455	264	36.08475	504	313	38.54237
T78_L122	59	501	328	49.7678571	591	402	51.07143	634	445	50.42857
T78_L123	62	204	128	35.2372881	339	266	47.37288	400	327	47.83051

T78_L124	59	210	101	26.6964286	316	208	28.94643	369	261	32.32143
T78_L125	61	426	249	35.4137931	554	347	39.39655	622	415	41.01724
T78_L126	50	186	117	33.212766	307	228	41.17021	355	276	42.80851
T78_L127	60	197	102	29.6140351	333	233	38.47368	421	321	38.47368
T78_L128	58	456	275	36.9636364	679	400	45.54545	734	452	49.49091
T78_L129	62	697	499	53.5423729	746	542	55	809	605	61.0678
T78_L13	58	372	245	43.5818182	498	342	47.27273	576	420	45.36364
T78_L130	62	489	322	50.2881356	589	432	48.76271	647	490	52.08475
T78_L132	58	334	150	31.8	445	265	33.83636	529	349	36.36364
T78_L133	57	491	279	41.1481482	578	338	39.53704	680	440	46.24074
T78_L134	55	227	104	31.0192308	452	249	42.84615	497	294	40.82692
T78_L135	58	304	186	31.7636364	413	263	39	469	312	43.09091
T78_L136	59	243	133	29.5	381	261	29.78571	465	345	32.30357
T78_L137	56	150	66	23.7358491	289	198	28.0566	368	277	27.79245
T78_L138	54	200	120	29.9803922	291	202	38.64706	365	276	42.80392
T78_L139	59	344	166	36.9821429	427	203	37.66071	469	245	43.23214
T78_L140	59	363	212	42.625	486	310	43.58929	523	347	45.05357
T78_L141	59	444	238	41.1607143	530	298	38.875	637	394	41.85714
T78_L142	48	191	106	26.9333333	463	325	41.88889	517	379	41.24444
T78_L143	57	539	278	40.0555556	877	495	47.42593	877	495	47.88889
T78_L145	62	480	290	41.4237288	602	407	42.0339	699	502	49.10169
T78_L146	57	271	138	34.037037	401	241	36.44444	454	294	39.92593
T78_L147	51	173	92	26.4166667	394	274	28.41667	482	362	31.1875
T78_L148	63	401	266	47.4666667	485	343	44.16667	575	433	47.38333
T78_L149	57	201	109	34.8518519	301	199	34.22222	351	249	35.07407
T78_L15	62	393	262	51.4576271	487	359	50.55932	554	426	52.40678
T78_L151	63	372	196	42.2333333	486	282	40.75	541	337	43.38333
T78_L152	52	160	84	19.9795918	370	220	29.69388	415	261	29.73469
T78_L153	45	159	74	29.1666667	335	205	31.21429	380	250	29.19048

T78_L154	60	321	160	33.2280702	483	301	32.98246	622	439	38.21053
T78_L155	62	305	171	37.9830509	453	315	43.59322	545	407	44.57627
T78_L156	61	738	447	53.3965517	752	449	48.65517	830	526	54.7069
T78_L157	55	125	58	18.4230769	267	186	22.44231	314	233	24.09615
T78_L158	60	278	121	35.7368421	351	197	39.21053	404	250	40.91228
T78_L159	56	311	193	38.5471698	533	394	47.09434	601	462	50.88679
T78_L16	45	138	82	22.7619048	403	285	41.35714	468	345	42.5
T78_L160	56	168	66	27.6415094	321	221	32.66038	375	275	34.24528
T78_L163	52	250	120	33.6734694	492	324	36.91837	588	412	45.28571
T78_L164	60	170	74	23.1578947	426	314	31.12281	525	413	37.7193
T78_L165	52	240	145	44.5102041	377	276	46.04082	438	337	50.42857
T78_L166	59	460	277	44.9464286	538	342	40.125	619	423	45.625
T78_L167	59	444	224	33.4642857	510	277	36.75	551	318	37.67857
T78_L168	58	204	128	36.3272727	314	237	40.09091	358	281	41.50909
T78_L169	54	374	191	37.9215686	601	385	46.68627	725	501	52.07843
T78_L17	57	381	217	39.8703704	550	348	44.81481	581	379	45.62963
T78_L170	55	267	136	29.8461539	482	299	36.03846	567	380	42.51923
T78_L171	60	313	166	33.7192983	448	288	33.36842	538	377	35.64912
T78_L172	60	311	150	28.8245614	431	267	31.36842	520	356	33.7193
T78_L173	62	217	110	32.0338983	308	197	33.33898	353	242	37.66102
T78_L174	57	176	95	24.5925926	418	301	32.25926	507	390	35.46296
T78_L175	57	499	312	41.3333333	792	522	49.77778	882	602	50.7037
T78_L177	60	251	147	36.5789474	351	255	38.10526	422	326	35.10526
T78_L178	57	338	206	37.037037	467	322	37.98148	524	378	40.87037
T78_L179	59	413	227	34.625	443	255	32.16071	486	298	34.875
T78_L18	56	260	125	34.2830189	437	295	41.09434	541	399	41.96226
T78_L180	56	395	268	46.3207547	419	295	49.62264	458	334	51.96226
T78_L181	58	184	110	24.3454546	379	259	28.85455	437	317	30.34545
T78_L182	57	387	215	49.6666667	502	324	50.87037	550	372	55.59259

T78_L183	58	220	102	28.8909091	400	281	41.23636	492	373	46.21818
T78_L184	56	387	242	43.5471698	562	371	47.15094	637	446	52.64151
T78_L186	54	210	116	30.0392157	366	247	34.94118	422	303	38.23529
T78_L187	58	207	87	28.9272727	348	220	30.43636	424	296	32.16364
T78_L188	57	350	241	37.037037	427	303	41.16667	493	369	41.68519
T78_L189	55	173	91	26.7307692	276	178	32.73077	327	225	38.17308
T78_L19	61	293	225	35.637931	439	366	40.72414	510	437	42.46552
T78_L191	58	372	207	32.7090909	515	333	34.83636	583	401	36.21818
T78_L192	53	210	83	24.62	382	202	28.04	443	255	28.22
T78_L194	64	478	291	48.1803279	599	406	47.60656	683	490	55.27869
T78_L195	61	173	72	24.5172414	230	127	27.84483	263	160	29.32759
T78_L197	59	380	226	38.8035714	531	353	39.32143	623	443	45.10714
T78_L198	56	170	83	26.5283019	405	309	38.15094	477	381	44.62264
T78_L199	56	247	114	26.1320755	376	235	25.66038	454	313	29.4717
T78_L2	63	561	385	43.8166667	679	492	52.91667	772	585	56.3
T78_L20	59	179	97	29.6428571	283	198	32.5	340	255	34.66071
T78_L200	57	250	153	37.4074074	425	325	38.92593	488	388	41.72222
T78_L201	61	300	151	37.4827586	438	267	38.31034	500	328	41.91379
T78_L202	58	340	221	42.8	394	261	43.10909	449	316	45.74545
T78_L203	58	548	371	53.0363636	668	487	56.87273	715	534	57.45455
T78_L204	53	456	310	44.8	552	406	42.66	602	456	44.38
T78_L205	59	214	111	34.25	367	223	37.375	408	264	41.28571
T78_L206	63	178	85	26.4666667	333	242	33.75	401	310	38.35
T78_L207	61	393	223	39.5344828	550	325	44.96552	617	391	47.2931
T78_L208	58	211	112	33.6727273	343	242	38.65455	395	293	38.87273
T78_L209	62	266	145	32.779661	423	282	39.98305	480	339	41.76271
T78_L21	57	198	84	25.9814815	308	187	30.48148	376	255	32.07407
T78_L210	47	173	92	30.9545455	500	323	43.75	575	398	47.97727
T78_L211	62	424	247	43.8983051	502	320	39.84746	573	391	42.72881

T78_L213	51	230	140	32.3125	358	247	30.54167	411	300	37.66667
T78_L214	58	397	262	47.0363636	487	327	46.16364	575	415	53.52727
T78_L215	55	196	116	33.3269231	317	217	42.26923	348	248	43.15385
T78_L216	62	242	150	33.220339	382	278	35.64407	460	356	35.77966
T78_L217	63	262	135	34.3166667	319	202	37.15	366	249	39.18333
T78_L218	48	229	122	25.9777778	852	590	47.57778	852	590	47.08889
T78_L219	60	262	174	31.3684211	412	307	33.03509	488	383	38.08772
T78_L22	63	590	293	38.9166667	693	387	38.58333	775	468	45.11667
T78_L220	59	305	152	39.2857143	419	232	42.53571	473	286	41.55357
T78_L221	59	185	88	26.4464286	326	220	28.375	399	293	29.82143
T78_L222	55	209	114	30.5576923	348	242	30.32692	398	292	30.76923
T78_L223	57	173	99	30.4259259	359	245	40.72222	436	320	42.94444
T78_L224	56	189	106	31.3207547	416	324	42.33962	500	408	44.4717
T78_L225	52	199	125	34.2040816	324	243	34.34694	369	288	35.4898
T78_L226	59	620	374	46.1964286	718	444	48.375	814	535	49.39286
T78_L228	51	283	178	36.2291667	366	262	37.3125	387	283	38.14583
T78_L229	61	319	172	32.7413793	443	290	36.43103	537	383	39.63793
T78_L23	58	234	105	31.8363636	361	229	33.94545	429	297	32.10909
T78_L230	62	263	147	36.6271186	396	270	36.11864	457	331	36.47458
T78_L231	63	278	152	31.0666667	453	296	33.1	543	385	36
T78_L232	61	461	283	43.4310345	546	361	44.46552	581	396	44.82759
T78_L233	63	588	414	45.3166667	545	372	42.98333	611	438	47.7
T78_L235	56	151	71	20.2264151	345	252	26.79245	432	339	29.22642
T78_L236	59	189	84	30.6428571	374	236	35.23214	468	330	40.14286
T78_L237	51	211	104	35.5833333	467	298	46	467	298	46.9375
T78_L238	58	168	83	32.7090909	423	303	46.83636	490	370	48.36364
T78_L239	54	213	109	30.3921569	329	214	39.52941	364	249	41.94118
T78_L24	62	745	498	45.9491525	723	476	43.16949	845	598	49.9661
T78_L240	52	157	83	23.4081633	354	243	32.34694	422	309	33.95918

T78_L241	55	293	169	34.5192308	390	252	34.71154	450	312	38.28846
T78_L242	52	167	87	31.6122449	311	207	40.26531	381	276	42.95918
T78_L243	61	217	124	35.637931	373	253	39.63793	451	328	44.82759
T78_L244	58	506	320	49.1454546	605	398	45.58182	648	441	49.61818
T78_L245	59	236	123	35.4464286	451	301	41.96429	504	354	43.64286
T78_L246	55	293	209	31.7692308	394	288	36.57692	449	343	41.71154
T78_L247	59	388	226	42.5357143	586	336	45.28571	639	388	48.60714
T78_L248	57	238	131	38.1851852	445	323	41.90741	445	323	42.14815
T78_L249	58	343	199	42.4909091	492	322	45.05455	576	399	49.56364
T78_L25	55	197	96	29.7307692	316	201	26.23077	407	292	27.13462
T78_L250	54	285	143	42.9803922	414	265	40.96078	503	354	39.52941
T78_L251	58	413	248	46.5818182	533	362	49.92727	643	472	55.32727
T78_L252	53	273	192	42.08	364	281	43.08	418	335	44.84
T78_L253	56	292	138	29.1132076	353	189	33.26415	422	256	33.49057
T78_L254	56	304	154	24.6226415	473	298	32.0566	576	401	32.09434
T78_L255	64	320	148	35.8360656	425	249	33.5082	552	376	49.88525
T78_L256	58	188	99	37.3454546	388	281	42.43636	463	356	45.38182
T78_L257	59	250	165	27.8035714	497	370	40.58929	566	437	46.73214
T78_L258	54	160	84	32.4901961	247	161	38.21569	297	211	37.80392
T78_L259	61	183	79	16.862069	441	251	26.96552	512	322	29.77586
T78_L26	51	183	88	31.8541667	310	208	34.02083	353	251	31.22917
T78_L261	52	263	152	38.2653061	433	264	42.77551	485	306	44.55102
T78_L262	61	266	147	40.9137931	373	245	41.58621	417	289	42.05172
T78_L263	55	156	80	28.7115385	334	246	28.67308	433	345	33.38462
T78_L264	52	197	101	31.3061225	374	252	41.97959	449	327	44.38776
T78_L265	60	437	243	42.9122807	604	388	45.45614	672	456	42.7193
T78_L266	53	306	179	35.94	489	346	43.98	489	346	45.26
T78_L267	57	262	139	32.462963	399	278	31.12963	472	351	35.87037
T78_L268	61	290	138	26.5172414	408	256	33.10345	480	328	35.93103

T78_L269	57	234	116	32.2222222	377	255	31.16667	436	314	33.57407
T78_L27	58	149	72	24.7454546	326	232	33.6	405	311	37.03636
T78_L272	55	302	177	47.9615385	435	296	48.17308	551	412	49.19231
T78_L273	64	435	249	42.7213115	500	310	43.03279	601	411	47.55738
T78_L275	64	281	150	33.9836066	397	248	35.83607	468	319	33.65574
T78_L276	60	250	135	32.0526316	402	265	36.08772	485	348	40.19298
T78_L277	60	209	130	29.754386	385	293	41.38596	463	371	45.31579
T78_L278	48	255	137	34.7333333	827	488	54.22222	827	488	55.28889
T78_L279	62	349	216	44.6779661	428	295	46.54237	487	354	51.77966
T78_L28	53	251	127	30.44	449	288	32.02	532	371	35.2
T78_L280	56	393	201	41.3207547	461	256	42.32075	595	390	47.43396
T78_L281	58	430	284	48.4363636	523	366	51.85455	596	439	53.10909
T78_L282	62	243	111	31.1694915	412	273	33.91525	494	355	37.0678
T78_L283	58	247	134	32.2909091	419	294	31.47273	498	373	33.03636
T78_L284	61	204	97	22.8448276	336	219	25.34483	440	323	27.06897
T78_L285	56	234	114	34.0188679	347	220	33.77358	394	267	36.13208
T78_L286	62	570	376	56.661017	678	482	52.49153	740	544	57.11864
T78_L287	62	583	381	45.7627119	595	393	44.9322	659	456	47.38983
T78_L288	56	369	216	39.2641509	487	297	38.39623	558	368	43.32075
T78_L289	53	165	91	28.82	337	259	40.12	407	329	44.4
T78_L29	59	317	160	31.1785714	394	224	32.92857	462	292	37.03571
T78_L293	62	338	195	46.0847458	425	268	48.50847	481	324	46.59322
T78_L294	55	181	99	28.5769231	413	308	40.36538	516	410	46.84615
T78_L295	57	237	133	33.1481482	303	192	34.66667	357	246	38.33333
T78_L296	60	378	183	38.4035088	558	341	46.52632	619	402	48.73684
T78_L297	62	234	116	27.3898305	384	265	32.45763	440	321	34.9661
T78_L3	62	666	445	41.2033898	720	456	36.13559	811	547	40.40678
T78_L30	58	303	196	33.6909091	445	322	38.96364	519	396	39.56364
T78_L300	47	151	81	30.9090909	298	213	32.22727	356	271	34.84091

T78_L301	64	351	227	42.4590164	436	312	43.85246	485	361	42.42623
T78_L302	57	239	136	38.2777778	341	235	39.35185	391	285	39.62963
T78_L303	53	296	185	38	475	361	41.5	534	420	41.56
T78_L304	54	172	117	31.0784314	492	410	51.01961	559	477	52.01961
T78_L305	56	469	321	37.4150943	586	414	36.88679	663	491	42.5283
T78_L306	61	318	170	39.362069	427	270	34.94828	471	314	39.10345
T78_L307	62	505	315	41.8983051	596	400	44.9322	710	513	44.61017
T78_L308	63	318	214	38.7833333	327	224	38	377	274	41.33333
T78_L309	57	259	137	31.7962963	400	264	32.55556	475	338	33.74074
T78_L31	60	189	77	26.4385965	353	238	34.87719	444	329	41.35088
T78_L310	61	226	126	33.5517241	379	273	33.62069	379	273	33.74138
T78_L311	61	482	324	42.5344828	635	448	47.41379	714	527	50.7931
T78_L312	54	483	358	54.1176471	700	537	61.52941	751	588	62.07843
T78_L314	61	751	443	43.3965517	859	544	43.60345	929	614	45.75862
T78_L315	57	417	271	56.0925926	520	350	56.90741	578	408	59.16667
T78_L316	53	193	85	24.8	367	219	36.36	435	287	37.28
T78_L317	56	162	83	20.3396226	329	233	29.84906	378	282	30.98113
T78_L318	62	324	194	33.4067797	457	334	32.30508	560	437	34.15254
T78_L319	52	194	111	30.3061225	387	298	39.40816	456	367	41.42857
T78_L32	60	168	96	32.5087719	262	193	34.36842	329	260	38.31579
T78_L320	57	191	107	32.1481482	332	237	37.83333	413	318	35.46296
T78_L321	59	301	190	41.5714286	433	318	48.83929	492	377	49.60714
T78_L322	49	243	138	31.1086957	525	363	46.36957	525	363	45.41304
T78_L323	64	603	409	53	634	431	49.52459	689	486	51.68852
T78_L324	51	375	246	44.0208333	583	407	48.54167	646	470	46.27083
T78_L325	59	381	254	37.8571429	451	319	38.48214	520	388	41.25
T78_L326	58	259	127	35.3090909	408	271	37.72727	493	356	37.56364
T78_L327	55	207	114	34.0769231	385	286	36.82692	470	371	42.57692
T78_L328	57	368	221	35.8888889	468	320	38.77778	567	419	40.87037

T78_L329	55	543	329	46.1923077	619	382	47.36538	642	405	50.01923
T78_L330	56	365	201	39.0377359	592	393	45.07547	723	521	53.79245
T78_L331	53	405	237	48.9	492	320	53.22	534	362	55.14
T78_L333	51	211	100	28.75	385	270	39.47917	421	306	42.97917
T78_L334	60	502	371	58.754386	635	479	61.59649	675	519	63.07018
T78_L335	57	356	192	46.9444444	575	376	53.42593	680	478	56.53704
T78_L336	61	666	417	53.7758621	798	532	60.56897	873	606	60.53448
T78_L337	55	304	158	45.6346154	418	233	45.48077	467	282	49.98077
T78_L338	58	616	347	52.5454546	659	341	46.41818	783	465	56.49091
T78_L339	55	351	212	45.6923077	515	372	51.69231	622	479	57.21154
T78_L34	60	228	122	28.4210526	370	257	28.45614	464	351	32.66667
T78_L340	54	228	142	29.0392157	382	268	31.01961	438	324	31.52941
T78_L341	49	169	84	26.4782609	396	246	31.76087	473	319	38.1087
T78_L342	54	367	170	37.3921569	511	298	38.21569	607	394	40.60784
T78_L344	54	241	136	33.6666667	330	224	38.03922	395	289	37.43137
T78_L345	60	295	171	37.1754386	415	278	43.10526	476	339	43.42105
T78_L346	57	200	89	30.3703704	363	247	32.37037	441	325	35.05556
T78_L347	59	200	92	28.0535714	329	215	28.14286	389	275	29.125
T78_L348	62	397	211	35.2711864	479	276	36.10169	555	352	38.83051
T78_L349	57	376	241	50.6296296	477	340	53.35185	529	392	55.01852
T78_L35	58	162	78	26.3636364	320	222	34.47273	372	274	37.03636
T78_L350	47	133	80	24.6363636	306	243	33.31818	396	333	33.13636
T78_L352	60	484	309	44.6140351	525	337	45.47368	592	404	49.57895
T78_L353	61	341	224	39.0517241	494	369	46.81034	573	448	48.68966
T78_L355	63	396	210	41.95	525	336	35.51667	616	427	34.81667
T78_L356	61	180	86	18.8275862	377	264	23.22414	474	361	26.7069
T78_L357	57	233	114	28.0740741	375	232	34.2037	459	316	38.94444
T78_L358	61	254	138	38.7241379	436	317	37.93103	525	406	44.37931
T78_L359	52	260	159	39.9795918	348	244	45.2449	375	271	48.20408

T78_L36	61	422	234	40.8275862	502	304	38.13793	589	391	42.60345
T78_L360	57	264	161	40.1851852	428	319	45.7963	496	387	47.55556
T78_L362	59	234	117	33.2321429	370	255	34.42857	453	338	37.98214
T78_L363	62	386	240	37.9152542	520	361	37.69492	621	462	42.33898
T78_L364	54	160	85	25.8823529	298	213	35.52941	336	251	33.80392
T78_L366	55	207	116	30.2115385	342	242	38.25	401	301	40.11538
T78_L368	57	279	117	29.2037037	396	206	29.18519	453	263	30.37037
T78_L369	53	221	130	30.44	471	335	36.7	593	457	41.7
T78_L37	53	182	105	35.48	389	311	40.2	491	413	44.2
T78_L370	58	296	133	39.6	391	213	36.29091	444	266	34.25455
T78_L371	62	285	150	35.1694915	418	258	36.91525	517	353	40.55932
T78_L372	63	290	176	37.1166667	444	320	36.78333	550	425	42.66667
T78_L374	56	316	186	42.509434	431	276	41.43396	508	353	45.28302
T78_L375	59	301	163	34.6428571	438	260	35.41071	542	364	43.42857
T78_L376	54	149	73	30.6666667	272	191	34.41176	309	228	37.43137
T78_L377	60	439	213	50.0526316	531	308	49.47368	627	404	51.92982
T78_L378	56	433	221	43.5849057	555	317	45.32075	618	373	48.4717
T78_L379	63	519	307	53.4	607	337	45.71667	698	423	49.13333
T78_L38	61	266	147	25.5	357	231	26.31034	408	282	28.01724
T78_L380	59	209	105	34.2857143	336	235	36.57143	407	306	38.21429
T78_L381	59	701	386	55.7142857	764	421	47.41071	834	488	50.625
T78_L382	55	281	125	36.4423077	529	277	40.25	621	359	43.11538
T78_L383	51	239	152	34.625	379	252	36.3125	423	296	37.75
T78_L384	56	298	181	39.5660377	424	292	44.15094	497	365	48.11321
T78_L385	52	179	101	24.4693878	397	310	35.53061	397	310	35.46939
T78_L386	56	301	197	38.3773585	479	359	43.83019	528	408	44.37736
T78_L387	52	255	152	35.6326531	405	276	38.97959	452	323	43.71429
T78_L388	59	539	320	47.0714286	740	485	54.42857	825	567	56.67857
T78_L389	60	396	236	34.4035088	679	436	34.35088	841	575	43.31579

T78_L39	55	318	177	35.0769231	452	272	40.44231	540	360	40.36538
T78_L390	59	221	117	30.6607143	350	247	36.07143	398	295	37.14286
T78_L391	51	169	91	26.1458333	339	249	34.0625	414	324	33.29167
T78_L392	46	205	139	42.5581395	465	352	55.46512	491	378	58.13953
T78_L393	60	304	180	37	359	228	36.77193	419	288	40.45614
T78_L394	51	139	66	27.7083333	376	289	32.3125	443	356	36.27083
T78_L396	56	448	284	43.6226415	540	353	43.88679	611	416	47.18868
T78_L397	56	224	121	33.6603774	384	268	43.26415	465	349	45.75472
T78_L398	59	181	86	23.3392857	295	202	32.39286	344	251	34.375
T78_L399	57	477	294	45.2037037	542	354	44.72222	585	397	47.59259
T78_L4	60	195	83	29.0877193	282	171	30.10526	325	214	32.92982
T78_L40	64	384	242	41.2786885	483	326	39.27869	597	440	40.2623
T78_L402	62	260	136	37.9152542	416	276	42.10169	500	360	46.35593
T78_L404	60	229	99	39.3157895	343	216	45.19298	404	277	43.05263
T78_L405	57	233	125	36.4074074	363	241	33.96296	443	321	36.07407
T78_L406	52	258	158	43.0408163	535	378	53.69388	592	435	55.42857
T78_L407	61	266	159	46.7068966	419	308	50.06897	485	374	51.05172
T78_L408	61	517	374	64.0862069	622	467	58.2931	697	539	64.58621
T78_L409	63	308	189	38.15	478	337	42.55	606	458	45.75
T78_L41	57	317	133	30.9074074	423	195	26.81481	546	312	36.51852
T78_L411	63	364	192	38.9833333	511	343	39.08333	622	454	41.85
T78_L412	59	299	182	29.9107143	411	296	31.33929	467	352	35.91071
T78_L413	58	180	92	23.1636364	293	203	25.78182	343	253	26.18182
T78_L414	53	257	135	32.38	419	266	41.68	485	332	42.92
T78_L415	62	270	148	43.2033898	465	294	47.89831	520	349	50.50847
T78_L416	60	389	231	36.2807018	522	353	40.26316	601	432	42.70175
T78_L417	58	426	249	32.0545455	467	266	35.23636	528	327	37.56364
T78_L418	59	607	306	38.6964286	645	310	36.875	716	377	41.16071
T78_L419	61	611	360	48.2758621	683	422	52.06897	763	502	54.12069

T78_L42	51	235	134	31.0833333	467	292	39.77083	535	360	39.625
T78_L421	57	263	131	28.6481482	414	278	32.88889	507	371	38.22222
T78_L422	59	303	136	30.9642857	449	233	31.30357	533	316	35.44643
T78_L423	64	530	316	40.8688525	556	311	38.34426	654	402	43.95082
T78_L425	54	182	119	27.8627451	370	274	32.03922	450	354	34.80392
T78_L426	49	195	106	28.5217391	543	367	45.15217	617	441	48.19565
T78_L427	60	553	331	47.7894737	595	363	45.5614	659	422	47.61404
T78_L429	57	254	148	32.9814815	353	245	41.77778	398	290	46.11111
T78_L43	58	290	168	43.7636364	448	314	46.67273	520	386	46.29091
T78_L430	61	285	183	36.7068966	469	373	38.77586	534	438	38.2069
T78_L431	56	313	173	40.8490566	488	321	41.39623	606	436	48.60377
T78_L432	57	203	89	30.4074074	299	181	32.7037	364	246	39.88889
T78_L433	56	155	72	23.6037736	312	229	28.20755	395	312	33.73585
T78_L434	59	321	200	37.375	495	361	43.73214	495	361	43.73214
T78_L435	57	356	200	41.0740741	439	273	36.98148	508	342	43.18519
T78_L437	55	427	230	35.8653846	557	317	42.40385	684	444	48.13462
T78_L439	58	164	74	28.2	295	203	33.72727	360	268	35.07273
T78_L44	58	486	202	36.5636364	477	183	34.09091	604	295	40.74545
T78_L440	50	192	119	25.1702128	365	276	35.55319	414	325	36.23404
T78_L442	60	478	327	47.4736842	630	470	52.01754	736	576	56.03509
T78_L444	52	131	71	18.7142857	326	247	24.02041	454	373	29.55102
T78_L446	61	250	144	30.3448276	412	283	32.96552	510	372	38.2931
T78_L447	57	242	114	23.9444444	356	217	29.42593	418	279	31.7037
T78_L448	61	478	300	44.5862069	543	363	46.27586	587	407	48.53448
T78_L449	53	333	193	33.54	432	280	34.76	477	325	37.6
T78_L45	61	531	301	48.3275862	636	381	42.17241	721	461	46.39655
T78_L451	53	149	70	25.4	284	202	29.62	322	240	29.2
T78_L452	53	576	394	55.34	685	492	55.1	757	564	55.54
T78_L453	60	327	176	35.8245614	437	277	37.57895	542	379	45.33333

T78_L454	58	366	213	40.5818182	510	346	43.67273	557	393	46.27273
T78_L455	62	215	108	26.3898305	279	165	27.62712	331	217	29.27119
T78_L457	50	194	90	28.2978723	378	251	38.70213	412	285	39.29787
T78_L458	57	365	187	44.3888889	436	246	46.77778	508	316	51.01852
T78_L459	51	169	100	33.4375	327	246	37.9375	403	319	41.41667
T78_L460	58	295	127	29.0909091	419	236	32.23636	492	309	35.12727
T78_L461	53	335	244	30.22	473	357	33.68	535	417	35.14
T78_L462	60	253	136	32.5263158	389	262	27.80702	463	336	28.87719
T78_L463	58	272	140	31.0545455	387	233	28.87273	479	319	34.8
T78_L464	56	326	181	42.7169811	487	300	40.32075	563	365	42.66038
T78_L465	55	179	90	28.0384615	308	212	31.90385	362	266	33.61538
T78_L466	49	240	146	30.8043478	485	326	39.17391	530	371	37.93478
T78_L467	57	408	255	42.8888889	583	413	45.88889	642	472	45.72222
T78_L468	61	462	255	40.7586207	523	314	36.7069	590	377	42.7931
T78_L469	55	210	119	28.3653846	338	241	30.32692	405	308	32.75
T78_L47	59	215	125	34.4107143	335	226	37.625	380	271	40.17857
T78_L470	48	146	82	23.8888889	280	208	34.75556	318	246	39.84444
T78_L471	59	384	221	39.625	530	294	35.82143	611	368	38.44643
T78_L472	48	192	68	24.1555556	329	171	22.37778	383	225	24.95556
T78_L473	63	570	396	56.45	595	410	54.05	661	476	59.15
T78_L474	58	178	85	25.7090909	363	259	30.25455	463	359	35.18182
T78_L475	58	321	200	34.0363636	410	289	36.92727	471	350	39.34545
T78_L476	45	114	64	17.5238095	408	298	30.97619	501	390	37.19048
T78_L477	47	209	117	35.7045455	443	302	47.56818	513	372	50.56818
T78_L478	61	328	197	46.4137931	416	284	44.24138	475	343	48.7069
T78_L479	61	534	324	47.0172414	701	487	51.62069	701	487	51.56897
T78_L480	55	226	119	34.7307692	390	261	38.28846	482	353	47.44231
T78_L481	61	451	237	36.1551724	521	290	33.10345	651	408	38.91379
T78_L484	59	468	240	42.6428571	495	268	38.21429	565	338	42.67857

T78_L49	45	145	68	35.7857143	882	510	56.97619	980	598	62.71429
T78_L491	55	326	173	36.4615385	519	336	36.34615	605	420	38.5
T78_L5	55	171	86	27.7307692	412	262	36.63462	484	332	42.40385
T78_L50	56	273	134	22.9622642	368	200	26.33962	437	262	29.49057
T78_L51	53	202	100	25.84	404	279	29.56	498	373	36.58
T78_L53	56	234	120	32.8113208	329	203	36.39623	385	259	39.16981
T78_L54	56	268	165	41.8113208	401	295	39.32075	473	367	42.24528
T78_L56	58	342	208	31.8545455	433	276	32.58182	509	345	32.69091
T78_L57	60	273	131	28.122807	423	274	31.4386	511	361	31.66667
T78_L59	59	166	78	26.0178571	325	234	29.44643	414	323	31.55357
T78_L6	60	500	256	43.7894737	501	250	40.4386	622	371	46.52632
T78_L60	60	500	305	41.3333333	596	371	47.31579	661	436	47.54386
T78_L61	51	218	118	32.8541667	381	238	35.79167	468	321	42.75
T78_L63	53	142	71	23.58	322	227	29.78	395	300	32.3
T78_L64	57	322	160	37.0925926	394	228	32.64815	455	289	36.87037
T78_L65	51	144	62	16.6666667	324	229	22.75	324	229	21.91667
T78_L66	58	224	89	26.1454546	391	250	36.03636	499	358	34.89091
T78_L67	59	237	145	39.6785714	408	308	45.64286	506	406	41.66071
T78_L68	56	223	121	26.6226415	411	302	40.13208	523	414	42.9434
T78_L69	58	573	380	53.8181818	650	459	54.61818	731	540	58.85455
T78_L7	59	235	95	29.9642857	380	222	35.01786	452	294	40.875
T78_L70	57	391	238	37.1296296	523	345	35.83333	586	401	37.22222
T78_L71	55	228	113	27.2115385	331	202	31.17308	424	295	33.90385
T78_L72	54	209	110	30.3529412	373	271	37.21569	450	348	40.47059
T78_L73	59	184	96	27.875	295	199	31.92857	365	269	35.03571
T78_L74	58	284	170	44.4727273	366	233	48.45455	401	268	51.85455
T78_L75	60	548	358	46.4561404	662	446	45.29825	718	498	47.21053
T78_L76	59	214	100	26.875	254	136	27.60714	308	190	32.01786
T78_L77	50	277	135	25.7021277	415	261	29.74468	488	334	31.51064

T78_L78	58	398	255	36	448	301	31.27273	502	355	34.63636
T78_L79	60	300	145	21.7719298	380	214	22.4386	414	248	22.98246
T78_L80	53	242	157	40.48	338	233	38.84	405	300	42.64
T78_L81	58	268	163	36.9272727	478	355	44.4	570	447	44.49091
T78_L82	58	159	88	40.7636364	245	174	39.98182	264	193	40.32727
T78_L83	60	138	70	22.1578947	288	213	33.40351	340	265	37.07018
T78_L84	58	251	122	28.0363636	393	238	33.41818	449	294	37.14545
T78_L85	61	412	214	35.5172414	521	309	30.7069	616	404	37.75862
T78_L86	49	232	106	26.173913	644	310	34.30435	744	410	35.04348
T78_L87	62	328	169	34.7627119	439	286	38.71186	537	384	40.08475
T78_L88	53	141	72	16.76	291	210	24.68	436	355	32.26
T78_L89	56	288	180	39	426	316	36.73585	518	408	38.15094
T78_L9	44	112	40	16.2195122	265	136	24.2439	306	177	32.87805
T78_L90	55	320	200	33.2692308	406	270	34.63462	472	336	36.03846
T78_L91	54	153	64	27.0392157	291	183	36.19608	356	246	38.64706
T78_L92	60	170	68	27.3684211	356	248	30.45614	464	356	34.26316
T78_L93	58	222	103	29	427	254	33.07273	519	341	34.36364
T78_L94	61	303	191	35.2586207	400	276	38.37931	468	344	41.25862
T78_L96	58	366	215	40.4545455	451	303	37.87273	514	366	44.10909
T78_L97	60	229	120	34.7894737	443	300	43.19298	533	390	46.14035
T78_L98	60	203	83	27.9298246	325	198	20.14035	423	296	25.05263
T78_L99	59	371	199	42.3035714	534	326	40.91071	615	403	43.16071